NASA CR-

ENERGY ADDITION METHODS

for

HYPER-VELOCITY TRUE FLIGHT SIMULATION

Arc Heater Department
Power Circuit Breaker Div.
Westinghouse Electric Corp.

CONTRACT NAS1-3629
TASK ORDER NAS1-3629-1
LANGLEY RESEARCH CENTER
NATIONAL AERONAUTICS AND SPACE ADMINISTRATION

SUMMARY

The work herein reported was performed by the Arc Heater Department, Westinghouse Electric Corporation for Langley Research Center, National Aeronautics and Space Administration under contract NAS1-3629 Task Order NAS1-3629-1.

The objective of this work was to define those modes of high power energy addition that appear feasible or promising for large-size wind tunnels. True flight simulation conditions with speeds from 12,000 to 24,500 feet per second and altitudes from 160,000 to 400,000 feet was the range of interest.

Two modes of energy addition, arc heating and magnetohydrodynamic accelerating, were found to be promising.

CONTENTS

SYMBOLS

a	acoustic speed
ac	alternating current
A	area
b	duct dimension
B	magnitude of magnetic induction
$\overline{B}$	magnetic induction
C	a constant
d	derivitive; duct dimension
D	diameter; characteristic length
dc	direct current
e	charge on electron
$\overline{E}$	electric field
f	frequency; cycles per second
$\overline{F}$	body force
h	specific enthalpy; convective heat transfer coefficient
I	current
j	joule
$\overline{j}$	current density
K	thermal conductivity; isentropic exponent; kilo (prefix)
L	duct dimension

m	meters
$\dot{m}$	mass flow
M	Mach number
MDH	Magnetohydrodynamics
MW	megawatts
n	voltage ratio
N_u	Nusselt number
p	pressure
p_{2t}	total pressure downstream of normal shock (impact pressure)
P	power
Pr	Prandtl number
R	gas constant
RF	radio frequency
Re	Reynolds number
S	specific entropy
T	temperature
u	internal energy; speed
$\bar{u}$	velocity
$\bar{v}$	velocity relative to main stream
V	volume
x	rectilinear coordinate

y	rectilinear coordinate
z	rectilinear coordinate
Z	altitude; compressibility
α	static to total temperature ratio at beginning of supersonic heating
β	ratio of heat added supersonically to energy prior to supersonic heating
δ	penetration depth
Δ	difference
η	efficiency
θ	Hall angle
λ	wave length
μ	dynamic viscosity; mobility
ρ	mass density
σ	electrical conductivity; parameter in the Bartz equation
τ	period (time between collisions)
ϕ	k/(k-1); heat flux
ω	angular frequency

Notes

1. An overscore (-) indicates a vector on average value of a scalor.
2. The subscript c indicates value at critical conditions.

1. INTRODUCTION AND MAJOR CONCLUSIONS

1.1 Introduction

The work reported upon in this document was performed by the Arc Heater Department, Westinghouse Electric Corporation for the NASA-Langley Research Center, Hampton, Virginia under Contract NAS1-3629 Task Order NAS1-3629-1.

The major writing was performed by J. B. Hammer and W. E. Franzen, and by S. Way of the Westinghouse Research Laboratories. The Project Engineer was J. B. Hammer. The Project Manager was A. Bruning. The Technical Representatives of NASA were W. E. Bruce, Jr. and R. R. Howell.

Information reported is based partially upon discussions and/or visitations to NASA-Ames, NASA-Langley, Arnold Engineering Development Center, Wright-Patterson Air Force Base, Johns Hopkins Applied Physics Lab, and Westinghouse Arc Heater Department.

The objective was to define those modes of high power energy addition that appear feasible or promising for large-size wind tunnels operating at conditions corresponding to true flight simulation at speeds ranging from 12,000 to 24,500 ft/sec (total enthalpies of from 3,000 to 12,000 Btu/lb) and total pressure of from 500 to 5,000 psi. Details of the operating ranges are shown in Figure 1.1-1. Stream power of interest in the task work ranged as high as 100 megawatts. To indicate more explicitly a possible range of mass flow, stream power, total enthalpy, flow rate, and total pressure the operating range of Fig. 1.1-1 is shown for a six foot diameter test core in Fig. 1.1-2. Modes considered included arc heaters, magnetohydrodynamic (MHD) accelerators, and high-frequency discharge heating.

1.2 Major Conclusions

The most significant conclusions arising from the study are as follows:

1.2.1 The operating range of interest considerably exceeds the performance capability of existing hardware.

1.2.2 Subsonic heating by an arc heater offers the most promising mode of energy addition for the lower enthalpy/lower pressure portion of the envelope.

1.2.3 Direct-current MHD acceleration, employing an electric arc as the pre-heater, offers the most promising mode of energy addition for the higher enthalpy/higher pressure portion of the envelope.

2. ENERGY ADDITION METHODS

2.1 Thermal Energy Addition Methods

2.1.1 Arc Heaters

Two configurations of arc heaters are presently receiving intensive study. One employs a long arc parallel to the fluid flow direction, and is hereinafter referred to as an "axial flow" arc heater. The other configuration employs a short arc normal to the fluid flow direction, and is identified as a "cross flow" arc heater. The two heaters will be discussed separately.

2.1.1.1 Axial Flow Arc Heaters

A typical axial flow arc heater arrangement is shown schematically in Fig. 2.1.1.1-1. These arcs are usually capable of adjusting their lengths over a rather wide range, with arc length influenced by mass flow and pressure level. In certain cases, however, the range of arc length is so small as to be essentially fixed by the electrodes geometry, as shown in Fig. 2.1.1.1-2.

There are two means of stabilizing the longitudinal arc. Each of these has been used successfully. The first method is to introduce a high degree of swirl to the incoming gas through a high-speed tangential gas inlet. Tangential inlets at large radii are helpful because they impart more angular momentum to the gas. This swirling action exerts two effects which tend to stabilize the arc. First, the swirl centrifuges the colder and more dense gas to the outside, thereby concentrating the hotter, more conducting gas toward the center of the arc. This maintains a central core of highly conducting gas for the arc to reside in. Second, the swirl establishes a radial pressure gradient such that the pressure is lower along the central portion. Since arc voltage decreases with decreasing pressure, the arc is inclined to remain in this central core. This swirl stabilization technique has proven very effective in operation. The major disadvantage of this scheme, compared with the constricted arc as described in the next paragraph, is the swirl effect in the arc heater effluent. Either a downstream stilling chamber must be used to damp out the swirl, or the swirl must be tolerated in the nozzle throat and test section.

The second stabilization method employs cold walls in close proximity to the arc. This is the "wall-stabilized" or "constricted" arc. The cold walls impose a low conductivity layer on the gas near the wall. This type of stabilization has been used effectively, and has the advantage of permitting a swirl-free effluent.

From theoretical analysis, however, both of the above arrangements are expected to have a highly non-uniform outlet temperature profile. This is the primary disadvantage in using heaters employing a longitudinal arc.

2.1.1.2 Cross-Flow Arc Heaters

A typical arrangement for a cross-flow arc heater is shown schematically in Fig. 2.1.1.2-1. In this type of heater, the arc length is usually much less than is found in axial flow arc heaters. Two advantages are projected for the cross-flow arc. First, the effluent gas issues from a reservoir inside the cylindrical surface described by the arc as it rotates; consequently it has a nearly uniform temperature profile in this reservoir volume. Second, the transverse arc lends itself more readily to multiple arc operation, a significant advantage when three-phase power is available. A typical three-phase arc heater geometry is shown in Fig. 2.1.1.2-2. Figure 2.1.1.2-3 shows an alternate arrangement for three-phase heaters which permits easier electrode spacing adjustment.

Both of these heaters may be operated as multiple arc direct-current heaters provided sufficient ballast is employed.

The geometries in Figs. 2.1.1.2-1, 2.1.1.2-2, and 2.1.1.2-3 have been successfully operated experimentally on alternating current. That shown in Fig. 2.1.1.2-1 has been operated on d-c also. The geometry of Fig. 2.1.1.2-3 is currently being built in 20 MW sizes and its performance should prove of significant interest in the arc heater field (2.1.1.1).*

2.1.2 High Frequency Discharge Heaters

One thermal energy addition method frequently proposed employs a high-frequency (RF) discharge. This method (shown for supersonic stream) corresponds to the schematic of Fig. 2.1.2. It has the advantage of not locating its electrodes in the gas stream. This eliminates a source of much gas contamination. Whether or not it provides a significant advantage depends on whether the electrode contamination constitutes a real problem. Early models of arc heaters produced highly objectional stream contamination; but newer arc movement techniques, better electrode cooling, and improvements in electrode material have reduced such contamination to the point where it is generally considered only a minor problem.

*Numbers in parenthesis in the text identify references cited in Section 10.

For effective heating, a RF unit must have a penetration depth as large as the heating volume radius. For large power units, this would be 1 to 10 cm. For air, the frequency, f, conductivity, σ, and penetration depth, δ , can be related by

$$\delta = 5 \times 10^3 / \sqrt{\sigma f}$$

or

$$f = 25 \times 10^6 \frac{\delta^2}{\sigma} \quad \text{cycles per second}$$

σ has a value of about 10 mhos/cm
For δ of 1cm and 10cm, this gives

$$f_{1cm} = 2.5 \times 10^6 \text{ cycles per second}$$

$$f_{10cm} = 250 \times 10^6 \text{ cycles per second}$$

These megacycle power supplies cost about $100/KVA. For a 100 megawatt unit, this amounts to $10,000,000 or 2 to 3 times the cost of a d-c supply. Spending several million dollars merely to reduce electrode contamination -- which is already at an acceptable level -- makes RF heating unattractive for this application.

In addition, RF heating introduces a very difficult engineering problem. The pressure vessel must either be made of low-conductivity material or segmented into many pieces. To date, a satisfactory pressure vessel has not been developed.

High-frequency discharge heating in the supersonic section is also not deemed feasible for the reasons discussed in Section 4.1.4.

2.1.3 Nitrous Oxide Combustion System

Figure 2.1.3-1 shows a schematic of one form of such a system. We are here interested in enthalpies of 3000 BTU/# (7×10^6 j/kg) and up. Such a technique at an equilibrium flame temperature of 1600°R starting from 540°R NO and N_2 yields air at only 360 BTU/# ($.84 \times 10^6$ j/kg) which is only a very small part of the total energy required. For this reason no further consideration will be given to this method.

2.2 Directed Energy Addition Methods

2.2.1 Direct Current MHD Accelerators

Acceleration of air by body forces makes possible the attainment of high total pressures at high total enthalpies, yet without actually subjecting any part of the flow system to extraordinarily high pressures. The body forces under consideration here are the Lorentz forces, arising from the cross product, j x B, of current density and magnetic induction, as might be provided in an MHD accelerator.

In the past, considerable attention has been focussed on MHD accelerator systems in which the current passes through the gas in the "breakdown" regime (2.2.1.1, 2.2.1.2). Although this type of accelerator may be of interest for space propulsion, its application for wind tunnels cannot be recommended due to the heterogeneous character of the output stream. Another type of MHD accelerator utilizes air as a partially ionized conducting medium. The conductivity is a function of the temperature and pressure, and is independent of the current in the range of interest. Such an accelerator has been under investigation by Messrs. Wood and Carter (2.2.1.3). A closed helium loop with cesium seeding, embodying an MHD accelerator of the equilibrium gas conduction type, has also been operated experimentally in Westinghouse laboratories (2.2.1.4). This latter type of accelerator lends itself quite well to theoretical analysis, with reasonable expectation of fair agreement between theory and experiment.

2.2.2 Traveling Wave Accelerators (AC MHD)

An arrangement for a traveling wave accelerator is shown in Fig. 2.2.2.1. Normally, all coils operate at the same frequency; requiring that the coil spacing increase in the downstream direction. If such spacing were not done, the ensuing slip (excess of wave speed over gas speed) would be unacceptable in some portion of the duct. Excessive slip results in excessive heating; while low slip results in excessive duct length for a given acceleration.

2.2.3 Self-Induced MHD Accelerator

Efforts in developing space propulsion techniques have produced a technological breakthrough in obtainable specific impulses. These high specific impulses correspond to extremely high enthalpies. The basic geometry of a self-induced MHD generator is shown in Fig. 2.2.3.1, although specific details of the accelerating process are not now known. Such devices have produced specific impulses of specific impulses of 7,000 sec. and 10,000 sec. (2.2.3.1, 2.2.3.2). The corresponding gas speeds and total enthalpies are:

Specific Impulse (sec)	Speed ft/sec	Total Enthalpy j/kg	Total Enthalpy Btu/lb
7000	225,000	2.3×10^9	1×10^6
10000	322,000	4.6×10^9	2×10^6

2.2.4 Electrostatic Accelerator

The arrangement of a typical electrostatic accelerator is shown in Fig. 2.2.4.1. A potential advantage of this system accrues from reduced joule heating since the electrons do not pass through the gas in the accelerating section. Theoretically, such an accelerator could function well at low static temperatures.

Development in this field may prove of interest for future test facility work.

3. STATE OF THE ART

3.1 Thermal Energy Addition

3.1.1 Arc Heaters

A sufficient number of arc heaters have been operated at combined pressure-enthalpy levels to make them of interest in present investigations of thermal energy addition. Unfortunately, in all cases where the pressure-enthalpy level was of interest, the power level, and associated mass flow rate, proved much below the value of interest.

Two generally different configurations of arc heaters were found to be of interest: the cross flow; and the axial flow. The latter employ two types of arc stabilization, namely: swirl stabilization; and wall stabilization.

Fig. 3.1.1-1 illustrates the "best" empirically limited performance determined during the course of the survey made for this study with all ratings and types considered together.

3.1.2 High Frequency Discharge

The present state of the art for high frequency discharge heating has attained pressures too low to be of interest here.

3.1.3 Traveling Wave Accelerator (ac MHD)

This device is relatively undeveloped, hence data is incomplete. Reported data leave room for doubt that the level of body force acceleration would be of interest to this program.

3.1.4 Self-Induced MHD Accelerator

Present interest in self-induced MHD accelerators centers primarily in the space propulsion field. As a result, measurements of flow distribution and gas properties have been neglected, with emphasis placed on thrust measurements. At present, the state of the gas stream is largely unknown.

Like the traveling wave accelerator, the self-induced MHD accelerator is as yet relatively undeveloped. Principal interest in this area lies in the enthalpies corresponding to the reported specific impulses of 7,000 sec and 10,000 sec; i.e., in enthalpies of 10^6 Btu/lb and 2 x 10^6 Btu/lb.

3.1.5 Electrostatic Accelerators

Electrostatic accelerators are in a very early stage of development, consequently there is no reported evidence of significant accelerator operation.

3.1.6 Direct Current MHD Accelerators

To date, direct current MHD accelerators have not been reported as operating at conditions at or near the envelope of interest here. However, present interest here is in the future developments of dc MHD accelerators.

3.1.6.1 Experimental Program at AEDC

The Arnold Engineering Development Center (AEDC) is now actively conducting an experimental program having as its ultimate goal the development of an arc heater-MHD accelerator combination capable of simulating essentially true flight with speeds ranging from 2,000 m/sec to 11,000 m/sec. Simulated conditions are 60,000 meters to 80,000 meters at 2,000 m/sec; and 80,000 to 130,000 meters at 11,000 m/sec on an altitude vs. velocity plot. To date, experiments have centered on seeded nitrogen, and have been aimed at the study of specific problems of long standing; namely, wind tunnel type operation, rather than merely demonstrating accelerators.

Discharge studies on seeded nitrogen, utilizing thermionically-emitting tungsten electrodes, have shown the difficulty of maintaining tungsten in the rather narrow temperature range between thermionic emission and melting of the electrode. Experiments have shown water-cooled cold copper electrodes as being more satisfactory in this application. However, certain problems may be encountered in long time operation with cold copper since it was noted that the seed material continually condensed on the electrodes.

Beryllia and pyrolytic boron nitride were found to be the best insulating materials for test section sidewalls and between electrodes. However, cooling of the boron nitride proved to be a problem, since no satisfactory method was found of bonding this material to metal for the transport of cooling water.

An experimental arc heater - MHD accelerator combination has been developed at AEDC. Designed for 1 megawatt output, the unit has a 2.5 centimeter square entrance, a 77 centimeter length, and a very slight divergence to accommodate boundary layer growth. The unit is provided with 117 pairs of electrodes, the central 60-pair being powered.

A 20-electrode-pair channel, corresponding to the upstream end of the experimental design, was constructed. Tests were performed at about 0.1 kg/sec flow of nitrogen seeded with about 1 percent potassium by weight. Inlet conditions were 1600 kcal/kg, 0.6 atm, and 2000 m/sec. The magnetic field was 1.6 teslas, and the $\omega\tau$ value for these tests was between 1.5 and 2.0.

Static pressure and exit impact pressure measurements were made on the above unit, and a velocity increase of from 20 to 30 percent was calculated based on the measurements. This increase proved somewhat greater than was anticipated. Accordingly, AEDC expects that the full 117-electrode-pair accelerator will be capable of more than doubling the gas velocity.

This accelerator unit is already in the construction and test stage of development.

3.1.6.2 Contracted Work for AEDC

In addition to the above in-house work, AEDC has contracted with the Avco Corporation to supply an MHD accelerator with approximately 20 megawatts output. Pilot operation of this unit will be as a tandem attachment to the output of a 20 MW three-phase arc heater to be supplied by Westinghouse.

4. FACTORS LIMITING PERFORMANCE

The discussion in Section 4 is confined to considerations of performance related to power level, combined pressure-enthalpy attainable, and efficiency. Basic problems are: gas containment; energy input to the gas; energy retention in the gas; and acceleration of the gas to suitable test section conditions. For the sake of convenience, heating is discussed separately from combined heating-MHD acceleration.

4.1 Heating

4.1.1 Gas Containment

The maximum total pressure of the present envelope of interest is 5,000 psi. For negligible speed heating and isentropic expansion to test conditions, this figure would correspond to a heater static pressure of the same value. Although this pressure alone does not constitute a serious containment problem, the difficulties of providing adequate gas confinement become appreciable when required gas temperature of from 4,700°K to 10,000°K are to be considered. Furthermore, if supersonic heating is employed, then the necessary heater pressure must greatly exceed 5,000 psi, as will be discussed later. No heater capable of operating satisfactorily at 5,000 psi was located in the course of the investigation. The state of the art curve (Fig. 3.1.1-1) indicates the possibility of providing 2,000 psi of air at 4,600°K. A significant advance in containment design must be achieved before the most demanding area of the envelope (5,000 psi and 10,000°K) can be attained.

4.1.2 Energy Input to Gas

Obtaining adequate energy input to the gas is usually a relatively simple matter. At least one possible situation, however, can present difficulties. For a fixed electrode gap, an operating range can exist wherein the arc characteristics result in a voltage/current product essentially a constant above a given amount, Fig. 4.1.2-1. (Below such a current value, the power decreases with decreasing current.) Hence for a maximum electrode gap and a given flow rate, nozzle size, etc., operation would occur on an arc-characteristic curve of maximum power. Here the power would increase with current increase until an operating level is reached such that the arc characteristics are given by

$$VI \cong \text{constant} = \text{power input}$$

Further increase in current will not result in a power increase until a very high current value is reached; when power will again increase with current. Unfortunately, current levels at which significant power increases may be expected are normally beyond the present capabilities of arc heater electrodes.

4.1.3 Energy Retention in Gas

A considerable amount of energy is lost between the time of its input to a gas and the time the impelled gas reaches the test section. Such a loss is reflected not only in lowered efficiency; it also contributes significantly to the ultimate combined pressure/enthalpy limit of performance. It is not presently known how much of such an energy loss is due to radiation and how much to convection.

As energy input to the gas is increased, one of two potential limits is ultimately reached. Either the power input limit is reached; or a ceiling is imposed upon ability to control losses due to limitations in chamber wall cooling. In either event, an inadequate performance limit is reached unless means of significantly reducing input power losses are provided.

There are two possible methods, for a given size, of reducing such energy losses. The convective loss can be reduced by ensuring that gas speeds are kept at a minimum consistent with mass throughput; i.e., keeping the Reynolds number at a minimum. This, however, requires avoidance of gas swirl. Alternatively, the combined radiation and convection losses could be reduced by utilizing a high temperature porous wall to obtain regenerative heating of the input gas. Determination of the effectiveness of either approach would require further investigation.

4.1.4 Acceleration of Gas

Maximum heat flux occurs in the region of the nozzle throat. Cooling in this area imposes serious limitations on gas acceleration. To date, a heat flux removal of about 40×10^6 Btu/hr ft^2 has been obtainable (at best) only through nucleate boiling.* Throat heat flux values for the operating envelope cannot be predicted with reasonable certainty.

---

*Non-boiling forced convection with water speeds in excess of 500 ft/sec holds promise of exceeding a heat flux of 40×10^6 Btu/hr ft^2. This belief is based on the familiar equation $Nu = 0.023\ Re^{.8}\ Pr^{.3}$. However, experimental verification will be required before sufficient confidence can be placed in such a prediction.

The employment of such schemes as transpiration cooling with gas and liquid, or with cold gas boundary layer injection, may prove necessary at the higher pressure/higher enthalpy conditions in the envelope.

A frequently proposed solution to the throat cooling problem is that of adding a large portion of the accelerating energy downstream of the throat. It is contended that this would permit the throat to handle gas of a much lower temperature, with (hopefully) a correspondingly significant reduction in the throat heat flux. Although such a proposal has not been exhaustively investigated, sufficient work has been done to indicate that such a technique holds little promise of providing practical values for significant parameters. This observation is substantiated in the following example.

> Consider two methods of heating for a test section simulating Mach 11 flight conditions at 166,000 feet. The first method (termed "Case A") would heat the air in a reservoir to simulate stagnation conditions at zero speed. The second method ("Case B") would add one-half the energy at zero speed; expand the air to supersonic conditions such that the static enthalpy is one-half that of the total enthalpy; add the rest of the heat supersonically at constant pressure; and, finally, expand the air isentropically to test section conditions. Details of the calculations involved are presented in Section 9.2 of this report, with only the results shown here. The required throat pressures and nozzle throat heat fluxes are as follows:

	"Case A"	"Case B"
Throat Pressure (atm)	142	822
Throat Heat Flux (Btu/hr ft^2)	9.6×10^6	12.4×10^6

> It is to be noted that supersonic heating produces a higher throat flux, due largely to the higher throat pressure.

4.1.5 Test Section Gas Dynamics

A limited amount of experimental data on impact pressure (P_{2t}), with less information on heat transfer rates and gas swirl angle, has been acquired.

W. B. Boatright (4.1.5.1) has reported some data on a 4-ft. diameter test section driven by a 10 megawatt cross-flow heater.

This data is reported in terms of Mach numbers as determined by measurements of impact pressure. A Mach number of 15.7 was measured at a point 3 inches above the centerline of the test section, with Mach 14.5 measured on the centerline. These measurements corresponded to a calculated stream core Mach 16.8. Boatright states (4.1.5.1) that this transverse Mach number gradient is too large to be attributable to source flow effects.

Work performed at NASA-Ames (4.1.5.2), employing Linde N4000 and N4001 heaters individually driving a 3/4-inch throat having a 24-inch exit and a 16-degree apex angle nozzle, has shown impact pressure as flat to ±10 percent over 30 percent of the test section diameter. These values were based on the test section diameter, and fell off quite rapidly outside this region. Heat transfer data reported on these units indicate heat flux imparted to a spherical segment-cylindrical probe as being flat to about ±13 percent over the central 30 percent. Flux decreased rapidly outside this region. The investigators (ibid) consider this data "preliminary".

Messrs. Smith and Doyle (3.1.1.5) experimented with a 7.3-inch exit, $M \approx 8$, 15-degree apex angle nozzle operating with 37 atm, 2560 Btu/lb stagnation condition. Air was supplied by a Linde N = 2 arc heater delivering 1 megawatt to the stream. These experimentors report an impact pressure survey as being flat to ±5 percent over the central 65 percent of the stream, based on diameter. They also report data showing swirl as being only a minor energy component in the test section. This conclusion could be expected on the basis of calculations based on angular momentum conservation. The same consideration leads one to expect a large increase in swirl angularity across a normal shock in the test section.

Velocity profile data has not been reported for any of the units in operation.

4.2 Gas Heating and MHD Acceleration

4.2.1 Containment

Containment problems associated with a heating and MHD acceleration combination center around the accelerator unit. Conversely, the reduced total pressure and total temperature requirements imposed upon the preheater (such as an arc heater) render containment in the preheater a relatively simple matter.

One containment problem peculiar to MHD accelerators, is the very high total temperature involved. Equilibrium conductivity enhanced by seeding currently appears the most promising solution to this containment problem. If this mode is employed, the accelerator inlet could be expected to operate at static and total conditions near those used successfully in existing MHD generators. However, total temperature in the exit region will be that of the test section; i.e., 10,000°K for the high speed end of the envelope.

It is to be expected that this temperature would induce severe heating of the duct walls in the downstream portion of the MHD accelerator. If use of hot ceramic walls is anticipated, since these have certain advantages over cold walls, then cooling of such walls may prove difficult in practice. There is, therefore, some as yet unknown total temperature which could not be adequately contained.

4.2.2 Imparting Power to Gas

Currently, the principal limitation on imparting sufficient power to the gas is that of introducing the power directly. It is desirable that a large portion of the energy to be imparted to the gas be added as directed energy by means of body force work, with only a minor portion to be in the form of thermal energy added by joule heating. It can be shown that the ratio of directed power to total power is essentially the same as the ratio of the counter emf (UB) to the applied field. This ratio, termed the "electrical efficiency", is occasionally identified as $\frac{1}{n}$, as in Section 5.2 of this report.

Since arbitrary control can be imposed over the applied field, corresponding control can be exerted over the electrical efficiency. In practice, however, selection of too high an electrical efficiency results in excessively long ducts, with frictional dissipation of the directed power. Thus the net efficiency can be very poor indeed. Section 5.2 of this report lists the effects of n selection, where choice of $\frac{1}{n}$ equals the electrical efficiency as noted previously. Without entering into detail, the practical limits of n may be stated as: $1.1 < n < 1.2$, approximately.

4.2.3 Energy Loss in the Gas

As noted in the previous Section, energy loss in the gas is primarily concerned with the loss of directed energy, which is one of dissipation to thermal energy. Such dissipation is due to viscous effects in the boundary layer. Correspondingly, the less the friction of the flow in the boundary layer, the less will be the energy dissipation. This fact leads to the use of either large cross section ducts; or to some forms of boundary layer control, such as by bleeding of the boundary layer.

Currently, the size of the MHD accelerator boundary layer is not precisely known. Therefore, or at least until further work is done in this area, it may be considered best to adopt the work reported by Wood (2.2.1.3) as indicating the minimum suitable duct size. Thus Fig. 16 in that reference indicates a boundary layer which may be considered marginal for facilities of interest in a one-inch-square accelerator. Thus one-inch may be taken as the approximate minimum dimension for a duct of practical value.

4.2.4 Pressure Gradient Acceleration of the Gas

Anticipated operating conditions in the test section are such that the MHD accelerator would be followed by a divergent nozzle section to provide acceleration to the gas. It is reasonable to expect that wall heat fluxes in this section would be about the same as those for a corresponding divergent section in a converging-diverging nozzle. This being the case, no particular difficulty with this section is to be anticipated. As a result, the gas expansion process is not expected to impose any serious limitations on test section operation.

4.2.5 Gas Dynamics in the Test Section

No experimental work reflecting the gas dynamics in the test section has been reported on expansion due to use of an MHD accelerator. Although no serious difficulties are expected, experimental work will be required to confirm this belief.

5. PROJECTED PERFORMANCE LIMITS

NOTE: Two systems--arc heaters and MHD accelerators--show promise for operation in the prescribed envelope. Each system is discussed separately below.

5.1 Arc Heaters

The presently reported state of the art curve (Fig. 3.1.1-1) is found to pass thru the lower enthalpy-lower pressure portion of the envelope. That some improvement in performance may be expected is obvious. Means are not presently available for accurately predicting just what the upper limit will become. However, for the case of axial flow constricted arc heaters, a procedure for establishing ultimate performance criteria is apparent.

Stine, Watson and Shepard (Ref. 5.1.1) of NASA-Ames have predicted performance of constricted arc heaters by a digital computer solution of the axially symetric flow equations. The validity of these predictions appears to depend primarily on the input data of gas properties. In particular, the radiation and thermal conductivity data are not now well known. Programs for gathering radiation data are currently active at NASA-Ames (inhouse) and for NASA-Langley (under contract). These programs should relieve the radiation data problem. With thermal conductivity as the remaining problem area, the following procedure should prove useful.

A heater of a size suitable for extensive testing (about 10 MW) could be designed with currently available conductivity data and the forthcoming radiation data. Such a heater would be experimentally tested so as to allow determination of the gross axial heat flux distribution. The discrepancy between the theory and experiment will indicate changes in input conductivity data. These new data may then be used as input for the computer program, although some iteration may be required. This extension of the Stine, Watson and Shepard approach should provide the means of predicting, as well as designing for, ultimate constricted arc heater performance.

Despite the fact that transport data is not available in the 100 atmosphere range to permit accurate results from such calculations, a preliminary result (based upon a heat flux containment limit) for a constricted arc axial flow unit has been developed, Fig. 5.1-1.

Prediction of a containment limit for a cross flow heater suffers not only from the same lack of high temperature and temperature transport data, but also from having such a complicated flow pattern that application of the Heller-Ellenbaas equations to this system is very difficult. However, a crude model has been developed in connection with contract NAS1-3629-3. Using these results the containment limit curve for a 62 MW heater shown in Fig. 5.1-1 results.

It can not be emphasized too strongly that both of these containment limit predictions in the region of interest can be in large error because of lack of arc radiation data.

5.2 MHD Accelerators

Consider MHD Accelerators using cesium seeded air as the working fluid. Tables I and II give compositions and properties of the equilibrium gas mixture at various temperatures and pressures. Calculations of chemical equilibrium follow well known thermochemical methods, using data from Ref. 5.2.1. Calculations of conductivity generally follow the lines of Ref. 5.2.2. Negative ions of the species O^-, NO_2^-, CN^-, and NO^- are considered in calculating electron density.

It may be argued that alkali-seeded air produces a "contaminated" stream in the test section. It is not the intention here to enter into all the aspects of the seeding question. However, a good case can be made for the use of seeding on the ground that in many (or most) wind tunnel applications, an air stream slightly contaminated with cesium is no more undesirable than an air stream provided from an MHD accelerator with alternative ionization procedures.

A map of the enthalpy-entropy field is shown in Fig. 5.2-1. In this Figure, a dot-dash boundary outlines the region of stagnation states corresponding to that shown previously in Fig. 1.1-1.

Certain points, (a) (b) (c) (d) (e) (f), are to be noted in Fig. 5.2-1. These represent stagnation states for cases that have been examined for application of the MHD accelerator. Enthalpy, entropy, pressure and temperature data for air are taken from Ref. 5.2.3.

In discussing the influence of such factors as pressure level and n-value, n is taken as the ratio of applied field to counter emf, uB. As noted previously, 1/n is a measure of the electrical efficiency of the accelerator.

The results for the six cases studied will be given for the n-value 1.15, which corresponds to an electrical efficiency of 0.869. Use of lower n necessitates closer control over joule heating losses, and does not contribute any advantages to generator design. Use of appreciably larger n leads to excessive values of the Hall coefficient.* For cases (a) (b) (c) (d), the pressure level in the accelerator was selected to give an inlet stagnation pressure (arc heater chamber) of 100 atm. In cases (e) and (f), inlet stagnation pressures of 7 atm were employed.

The inlet and outlet areas A_1 and A_2 correspond to a test section area $A_3 = 2.605\ m^2$ (28.3 ft^2, 6 ft diameter core for which total data is presented in Fig. 1.1-2). This is the area assumed for the comparisons discussed in Section 6 of this report. It may be desirable to alter A_1, A_2, A_3 proportionately to achieve a larger test section or larger accelerator cross sections.

---

*This comes about because the accelerator inlet temperature is reduced as n is increased, hence mean conductivity is reduced and B is increased to maintain a given length. As a result, the product μB increases.

The choice of n-value, then, may be summed up as follows:

Starting with n close to unity, increase of n will at first exert no adverse effect by causing a large Hall coefficient; but eventually, at around n = 1.20, the Hall coefficient begins to increase rapidly. Increase of n, with constant p_1, p_2 and p_{1t}, will

decrease T_1
decrease T (average of T_1 and T_2)
decrease σB^2
decrease s_1

The situation regarding choice of pressure level is as follows:

Decrease of p_1 and p_2 with specified p_{1t} will

decrease s_1
decrease T_1, T_2, T
decrease σ
increase μ
decrease σB^2
increase μB
increase A_1, A_2, d_1, d_2
have a favorable effect on heat loss and friction losses.

It is desirable that the lowest pressure level be used which is acceptable from the standpoint of the magnitude attained by μB. This quantity should preferably be kept below 10; or, even better, below 8.

Table III presents the data for the six cases. Reference may be made to Figs. 5.2-2 and 5.2-3 for notations.

It is seen from Table III that wide variations occur in the required electric power (for the accelerator), P_E: ranging from 22,500 KW in case (a), to 1.82 KW in case (d).

In order to operate an MHD accelerator for altitudes as low as that of case (a) namely 250,000 ft., a high pressure level, such as 1 atm, must be employed in the accelerator. If an appreciably lower pressure were used, the temperature in the accelerator would be too low and conductivity would be adversely affected.

At very high altitude conditions the appropriate pressure in the accelerator is quite low, being about 0.01 atm. Higher pressures lead to very small duct dimensions and appreciably higher gas temperatures. Still lower pressures than 0.01 atm would lead to excessive μB values. The difficulty encountered at test section simulated altitudes of 400,000 ft. and over is that the area of the accelerator duct section is very small, unless the test section area is very large. Thus, for case (d) we find for $A_3 = 2.605\ m^2$ the dimension $d_1 = 0.008$ m. To obtain a bigger duct, the entire wind tunnel must be built to larger scale; else an appreciable fraction of the flow must be wasted.

It might be possible for the test section conditions represented in cases (e) and (f), and the corresponding stagnation conditions, to be reached by arc-heated wind tunnels of future design, going beyond present day attainments. In any event, the relative difficulty of the two approaches, for case (e) for example, may be compared as follows:

	Arc Heater	MHD
Arc chamber p:	63 atm	7.0 atm
Arc chamber h:	5450 Btu/#	3240 Btu/#

By designing the MHD accelerator to run at 1 atm pressure it appears possible to simulate altitudes in the test section as low as 200,000 ft.

The foregoing discussion relates to the potential core of the flow. Since friction and thermal boundary layers will exist along the test section walls, the actual duct area must be large enough to provide the gas for these layers, in addition to the potential core. Wall and electrode constructions may be envisaged to keep gases of high stagnation enthalpy away from the walls. Any discussion of accelerator construction concepts, however, lies beyond the scope of this report.

It may be stated, then, that the MHD accelerator appears applicable to all conditions represented all six cases (a) . . . . . . (f). Only the lower left portion of the dot-dash region shown in Fig. 5.2-1 is considered doubtful for MHD accelerator application.

It will be noted that Table III indicates p_{1t} pressures as considerably below those of p_{3t}. In other words, the pressure required in the arc heater chamber when the MHD accelerator is used is considerably below that required were the heater to discharge directly into the accelerating nozzle and test section. Attainment of high chamber pressures at high stagnation enthalpies, however, generally poses difficult problems where good durability, low contamination, stream homogeneity and prolonged operation are desired. Consequently, there can be a real advantage in pursuing further development of an MHD-DC accelerator.

It is also to be noted that the velocity ratio for the accelerator necessary to realize the advantages inherent in its use is generally not large, being in the range of 1.1 to 1.5.

TABLE I

Air and 0.005 Cesium by Weight

Mole Fractions

T °K:	2300°		2500°		2700°		2900°	
p atm:	.01	.05	.01	.05	.01	.05	.01	.05
CO	.000063	.000032	.000140	.000083	.000208	.000154	.000241	.000211
CO_2	.000233	.000267	.000151	.000213	.000073	.000137	.000028	.000070
N	.000000	.000000	.000002	.000001	.000014	.000006	.000058	.000027
NO	.015438	.015762	.020755	.022026	.024231	.027940	.023781	.031626
NO_2	.000002	.000004	.000001	.000004	.000001	.000004	.000001	.000003
O	.021441	.009762	.058163	.027396	.125071	.063523	.209990	.122217
A	.009388	.009444	.009213	.009360	.008896	.009188	.008492	.008909
N_2	.763349	.767749	.746346	.757724	.718496	.740657	.685575	.715900
O_2	.189007	.195896	.164170	.182118	.121988	.157337	.070860	.120014
C_s	.001078	.001085	.001058	.001075	.001022	.001055	.000975	.001023

	2300°		2500°		2700°		2900°	
	.10	.15	.10	.15	.10	.15	.10	.15
CO	.000023	.000019	.000064	.000054	.000128	.000113	.000190	.000176
CO_2	.000276	.000280	.000233	.000243	.000165	.000181	.000096	.000112
N	.000000	.000000	.000000	.000000	.000004	.000004	.000019	.000016
NO	.015840	.015875	.022341	.022482	.028927	.029378	.034024	.035165
NO_2	.000005	.000006	.000005	.000007	.000005	.000007	.000005	.000006
O	.006932	.005670	.019612	.016101	.046310	.038328	.092300	.077615
A	.009457	.009463	.009397	.009413	.009270	.009308	.009051	.009121
N_2	.768819	.769294	.760611	.761912	.746882	.749774	.726373	.731533
O_2	.197562	.198305	.186657	.188705	.167244	.171838	.136902	.145207
C_s	.001086	.001087	.001079	.001081	.001065	.001069	.001040	.001048

TABLE II

Air and 0.005 Cesium by Weight

Electron Mobility and
Electrical Conductivity

	μ, $\frac{m^2}{\text{sec volt}}$	σ, $\frac{\text{mhos}}{\text{m}}$
2300°K		
.01 atm	92.686	69.587
.05	24.235	39.153
.10	13.375	27.214
.15	9.399	20.762
2500°		
.01	76.429	115.34
.05	20.766	76.259
.10	11.661	59.810
.15	8.287	50.431
2700°		
.01	67.155	161.38
.05	18.083	121.22
.10	10.244	101.30
.15	7.324	89.55
2900°		
.01	65.209	197.68
.05	16.454	167.61
.10	9.256	147.48
.15	6.615	134.57

TABLE III

Case Data for Figure 5.2-1

	Case (a)	Case (b)	Case (c)	Case (d)	Case (e)	Case (f)
Alt. ft.	250000	300000	350000	400000	300000	400000
Speed, m/sec	5000	6000	7000	8000	5000	7000
S_3/R	33.20	35.83	39.15	42.40	35.83	42.40
T_3 °K	196	195	242	385	195	385
h_3 j/kg	195200	185000	242000	386000	185000	386000
10^6 p_3, atm	20.07	1.249	0.1121	0.0211	1.249	0.0211
h_{3t} x 10^{-6} j/kg	12.695	18.185	24.742	32.386	12.685	24.886
p_{3t} atm	570	490	275	190	63	31
n	1.15	1.15	1.15	1.15	1.15	1.15
p_2, p_1 atm	1.00	0.15	0.05	0.01	0.15	0.01
S_1/R	32.38	34.75	38.34	41.80	35.00	41.53
T_2 °K	2800	2880	3165	3300	2880	3300
T_1 °K	2470	2585	3030	3100	2670	3087
ρ_2 kg/m3	.1243	.01775	.004975	.000899	.0177	.000899
ρ_1 kg/m3	.143	.02125	.00534	.000975	.0195	.000984
A_2 m^2	.00888	.000396	.000097	.0000634	.000424	.0000666
A_1 m^2	.01049	.000429	.000104	.0000638	.000560	.0000734
10^{-6} h_2 j/kg	3.61	4.18	6.043	7.35	4.19	7.35
10^{-6} h_1 j/kg	2.99	3.33	5.325	6.76	3.52	6.52
d_2 m.	.0942	.0199	.00985	.00796	.0206	.00816
d_1 m.	.1024	.0207	.0102	.00799	.02366	.00857
u_2 m/sec	4260	5290	6115	7080	4120	5925
u_1 m/sec	3140	4080	5275	6495	2835	4900
p_{1t} atm	100	99	100	99	7.0	7.4
10^{-6} h_{1t} j/kg	7.925	11.665	19.234	27.866	7.545	18.526
$\bar{T}$ °K	2635	2732	3097	3200	2775	3193
$\bar{\sigma}$ mho/m	40	96	215	233	106	232
$\bar{\mu}$ m^2/volt sec	1.2	7.2	15.5	67	7.05	66
B web/m^2	5.06	1.288	0.378	0.1245	1.22	0.1644
$\bar{\mu}$B	6.08	9.27	5.86	8.34	8.60	10.85
L m.	1.00	1.00	1.00	1.00	1.00	1.00
u_2/u_1	1.358	1.296	1.16	1.090	1.453	1.208
m kg/sec	4.71	.0372	.00295	.000404	.031	.000354
P_E KW	22,500	242.5	16.25	1.823	159	2.25

6. COMPARISON OF ENERGY ADDITION METHODS

6.1 Basis of Comparison

For the purpose of comparison, a single operating point will be considered. The chosen condition corresponds to true flight simulation at 166,000 ft. at a Mach number of 11. A six-foot diameter stream is assumed. For this condition, the pertinent quantities are:

$$Z = 166{,}000 \text{ ft}$$

$$M = 11$$

$$\frac{S}{R} = 30.77$$

$$p = 7.31 \times 10^{-4} \text{ atm}$$

$$p_o = 222 \text{ atm}$$

$$T = 270.65^oK$$

$$T_o = 4600^oK$$

$$\rho = 5.95 \times 10^{-5} \ \#/ft^3$$

$$\rho_o = 1.018 \ \#/ft^3$$

$$a = 1082 \text{ ft/sec}$$

$$u = 11900 \text{ ft/sec}$$

$$h = 117 \text{ Btu/\#}$$

$$h_o = 2950 \text{ Btu/\#}$$

$$\dot{m} = 20.0 \ \#/\text{sec}$$

$$P = 62.2 \text{ MW}$$

6.2 Comparison of Most Promising Methods and Required Advances

The most promising systems for energy addition are axial flow arc heaters; cross flow arc heaters; and MHD accelerators. Present performance data pertinent to this operating point (true flight simulation at Mach 11 and 166,000 ft.) are shown in Table IV following.

TABLE IV

System Performance Data

Remarks	Foot-note	Stream Power MW	Stream Power %	Total Pressure atm	Total Pressure %	Total Enthalpy Btu/#	Total Enthalpy %	Effi-ciency %
required conditions	-	62.2	100	222	100	2950	100	-
axial flow arc heater	1	.15	.25	100	45	4000	136	41
" "	2	1.8	2.9	67	30	3310	112	46
" "	2	2.4	3.9	44	20	3840	130	51
" "	1	.13	.21	20	9	9900	346	44
cross flow arc heater	3	1.2	1.9	100	45	2700	92	26
MHD accelerator	4	.2	3	~2	1	17200	580	60

1. Linde 1/4-MW Heater (Ref. 6.2.1)

2. Linde N-4000 (Ref. 6.2.2)

3. Westinghouse 10-MW Heater (Ref. 6.2.3)

4. NASA-Langley 2.5 cm Accelerator (Ref. 6.2.4)

As will be noted from the above Table, none of the units cited are in the required power range. Pressure levels are limited to about half that required. The arc heaters have operated near the required enthalpy at half the required pressure.

The largest advance required in the state of the art is obviously an increase in the power level by an order of magnitude or more. Performance predictions based on scaling (by size only, not enthalpy level) by the required factor of 20 or 30 cannot be made with suitable confidence at this time, although some scaling laws have been developed on an empirical basis (Ref. 6.2.5). These laws appear to be somewhat incomplete and their validity for scaling by a factor of 10 or more has not yet been established. They are, however, the best presently available. Should these rules of scaling prove valid, or if they can be modified so as to become valid for the 50 MW heater under construction (Ref. 6.2.5), this would be very significant to the high power-high speed facilities of interest in this contract. Acceptable scaling predictions for axial flow heaters and MHD accelerators will likely precede those for cross flow heaters because of good mathematical models. How well these models will predict performance will need to be determined from additional work.

A second major step to be taken is an increase in pressure. Pressure containment at 222 atm presents no real problem. Attaining 2950 Btu/# at a pressure above 100 atm is presently possible, 100 atm and 4000 Btu/# having already been reached.

An improvement in efficiency, although highly desirable, does not appear attainable with the present cold metallic wall. Development of a regeneratively cooled high temperature wall may provide a significant increase in efficiency.

6.3 Ultimate Performance Limit Comparison of Axial and Cross Flow Arc Heaters

As has been mentioned several times, controversy exists as to the relative merits of the cross flow and the axial flow arc systems. Proponents of the cross flow system have proposed as its virtue a "uniform" thermal cross section to the nozzle. At the same time there has been no evidence that such a unit can be operated above the experimental 3000 Btu/#, 100 atm limit.

Proponents of the axial flow concept have proposed as its virtue the ability to reach much higher enthalpy-pressure conditions based upon well developed theory, and less well developed fundamental transport data. At the same time such an approach has developed theoretical data which indicates the thermal profile will be very non-uniform under some conditions of interest.

In this comparison between the two concepts reference 6.3.1 presents a qualitative model from which the conclusion for the cross flow arc is drawn that "little hope exists for achieving high values of enthalpy in the core at the test section* because most of the heat is received from the relatively cool aureole."

*Stine, H. A.; The Hyperthermal Supersonic Aerodynamic Tunnel, Int. Union of Pure & Applied Chemistry, Butterworths, London, 1964.

This study should, if possible reach conclusions concerning the possible potential comparative performance of the two types of arc heaters. Since no one has tried to quantitatively project the possible upper limit of a cross flow arc system for comparison to the axial arc, this is the first step in this process. Fig. 6.3-1 qualitatively indicates a thermal profile calculated for a typical cross flow arc heater. Based upon this configuration work in connection with NAS1-3629-3 (5.1.3) has calculated heat losses for such a unit. Fig. 5.1-1 indicates a comparison between the cross flow and an axial flow containment limit.

Based upon these comparisons (between different ratings) one would conclude that

1. The axial flow system can reach a higher peak enthalpy, ignoring profile considerations and rating influence (it is this that prompted the original plasma jet work by Siemens Schuckert in the 1930's to develop a radiant lamp source to pursue this technique).

2. The cross flow system, if it is indeed "more" uniform in thermal profile, has not been developed to the limits.

3. In the high pressure regime, particularly, development of arc hardware should lead to coverage of a much greater proportion of the envelope of interest to NASA.

7. CONCLUSIONS

NOTE: The following conclusions are based on: a) an examination of the literature; b) engineering calculations; and c) examination of facilities and discussions with personnel working in this field at NASA-Ames, NASA-Langley, Arnold Engineering Development Center, Wright-Patterson Air Force Base and Westinghouse Electric Corporation.

7.1 The minimum required enthalpy of 3,000 Btu/# for the operating envelope has only been achieved at pressures up to 100 atm and then at a power of 1/4-megawatt (Ref. 7.1.1).

7.2 The maximum power of any existing unit potentially capable of operating in any part of the envelope is 5 megawatts (Refs. 7.2.1, 7.2.2).

7.3 Arc heaters have operated satisfactorily in the low enthalpy and medium to low pressure portion of the envelope.

7.4 There is no known technological reason why the arc heater's capability cannot be further extended into the higher pressure-higher enthalpy region of the envelope.

7.5 The present state of the art for arc heaters falls so far short of the high enthalpy-high pressure part of the envelope that it is very unlikely that arc heaters can cover the entire envelope.

7.6 MHD acceleration appears unnecessary over the low enthalpy portion of the envelope.

7.7 The ultimate performance limits of MHD accelerators lie outside the region of interest here; consequently MHD accelerators can cover that portion of the envelope not covered by arc heaters.

7.8 The state of the art of Self-Induced MHD is not sufficiently developed to allow a reliable prediction of its application to wind tunnels; however, the high enthalpies obtained with this device are of interest.

7.9 Electrostatic acceleration is unattractive because no clear advantages over MHD exist and the technical problems of charge production and charge neutralization have not yet been solved.

7.10 High frequency discharge heating is unattractive because no clear advantage exists over arc heating; the cost of the power supply is considerably greater; and the art of hardware development is not as well developed.

7.11 Traveling wave pumps (alternating current MHD) are presently unattractive because of lack of development and lack of operating flexibility in a given piece of hardware.

7.12 Nitrous oxide combustion is unattractive because of the low enthalpies obtainable.

7.13 Supersonic heating in any form is unattractive because of its failure to relieve the nozzle throat cooling problem and its severe upstream total pressure requirements.

7.14 Accuracy of air radiation and conduction properties are the principal limiting factors on predicting the upper limit of performance of axial flow arc heaters.

7.15 The principal factor limiting the accuracy of predicting the upper limit of performance of cross flow arc heaters is the lack of a suitable mathematical model.

7.16 For heaters within or near the present state of the art, prediction of performance limits for axial flow heaters will continue to be more accurate than those for cross flow heaters due to the complexity of the flow and heat transfer in cross flow heaters.

7.17 The experimentally determined performance of axial flow heaters is superior to that for cross flow heaters. In terms of maximum pressure and high enthalpy (100 atm and 3,000 to 4,000 Btu/#) and in terms of low pressure maximum enthalpy (1 atm and 5,000 to 30,000 Btu/#) the axial flow heater is slightly superior. In terms of efficiency, the axial flow heater is markedly superior.

7.18 The major factor limiting arc heater performance is the maximum allowable wall heat flux of 40×10^6 Btu/ft^2 hr.

7.19 Swirl in the test section resulting from swirl in the arc heater is quite low in the free stream but may be of concern downstream of model induced shocks.

7.20 Measurements to date of test section thermal and velocity profiles are very rough and are inadequate for an accurate and reliable statement of these important test section properties.

7.21 The theoretical treatment of MHD accelerators is more highly developed than that for arc heaters, but the hardware development of MHD accelerators is far behind that for arc heaters.

7.22 The maximum power of heaters presently under construction is 65 MW.

7.23 Significant MHD acceleration has been achieved, but only at conditions far removed from true flight simulation within the operating envelope of interest here.

7.24 There is a minimum size for which MHD devices can be used for small scale experiments. Below this size, boundary layer effects are disproportionate and results cannot be scaled. A practical minimum size for studies of a 100 MW unit is in the 10 to 100 megawatt range.

7.25 A strong difference of opinion exists as to the merits of seeding in MHD accelerators. Reliable investigators report that less non-equilibrium energy exists in the seeded air at the test section. Catalytic effects of seeding are not known.

7.26 The upper limits of arc heater performance have been predicted, and are shown to exceed the entire operating envelope in terms of pressure and enthalpy.

7.27 One axial flow arc heater, built after careful design, has performed at low pressure at conditions significantly in excess of the then state of the art.

7.28 No high pressure arc heater, either axial or cross flow, has been built using the presently available best analytical basis for design.

7.29 An axial flow-constricted-arc heater designed on the basis of the best available analytical approach would have an excellent chance of meeting the maximum pressure-minimum enthalpy requirements of the envelope as well as some of the lower pressure-higher enthalpy part of the envelope.

7.30 A cross flow heater, on a theoretical basis, should have more uniform thermal profile than an axial flow unit.

8. RECOMMENDATIONS

8.1 That portion of the operating envelope which can be covered by an axial flow constricted-arc arc heater of high power should be accurately determined. This can be accomplished by a three-step program as follows:

8.1.1 Design a 100 MW heater and obtain performance predictions based on a digital computer solution of the radially symmetric flow equations. This would follow the method of Stine, Watson and Shepard (Ref. 8.1.1.1) of NASA-Ames, but would not be limited to this model.

8.1.2 Repeat this step for a heater of 10 MW size.

8.1.3 Construct and experimentally test the 10 MW heater to determine the accuracy of the computer solution for heater performance. Data from this program will suggest improvements in input data for the foregoing steps. If the accuracy of prediction is not initially satisfactory, reruns of the first step and the performance prediction part of Step 8.1.2 may be desirable.

8.2 The critical problem areas of high power direct-current MHD accelerators should be defined and solutions sought. This accelerator would be one suitable for operation in the high enthalpy - high pressure part of the operating envelope. Proper steps for accomplishing this are as follows:

8.2.1 Detail design a large power MHD accelerator for operation in the high enthalpy - high pressure part of the envelope.

8.2.2 From the design of this first step, define the critical problems of actual manufacture and operation.

8.2.3 Solve those problems of Step 8.2.2. Solutions will probably be arrived at from experimental work on components of the accelerator, combined with design ingenuity.

8.2.4 Incorporate the results of Step 8.2.3 in the original design of Step 8.2.1 From this final design, determine if it is feasible to use a MHD accelerator.

8.3 Understanding of radiation processes from high pressure arcs is an absolute requirement before enthalpy scaling of arc heaters can be accomplished. This program should consist of:

8.3.1 A theoretical calculation of radiation emission and reabsorption for arbitrary Planck source functions should be performed.

8.3.2 Spectral data for a well defined configuration should be collected to permit determination of the Planck source functions.

8.4 A search for theoretical insight into the cross flow heater should be continued because of its potential superior profile. When reasonably accurate transport data are available a comparison of optimized axial flow and cross flow units of the same rating should be made. Such a comparison at the present time is not warranted in view of the lack of high pressure radiation data and a confirmed theoretical model of a cross flow heater.

9. APPENDIX

9.1 Measuring Systems

9.1.1 Mass Flow

Measurements of the mass flow rates of the gas to be heated are presently being made either by means of subsonic sharp-edged orifices, with sonic nozzles; or with supersonic nozzles. (Turbine meters are outside the experience of the authors.)

Subsonic* sharp-edged orifices have been employed extensively in low pressure system measurements. Accuracies are about 5% for uncalibrated units, and about 1% for systems calibrated at or near the operating conditions of pressure, temperature and flow. Some investigators report using the subsonic approach in measuring high pressure systems common to arc heater operation. At higher pressures, the problem of differential pressure measurement becomes more acute since such measurement is intimately involved in the flow calculation. This factor is shown in the following equation, where

$$\dot{m} = C \sqrt{P \Delta P / T}$$

Representative values for the variables in the above equation are: $P = 3000$ psi; $\Delta P = 5$ psi; and $T = 530^{o}R$. Although measurements of P and T are made readily, the measurement of 5 psi in a system operating at 3000 psi presents real difficulty. In some systems, the device for measuring a ΔP of 5 psi is exposed to a ΔP of nearby 3000 psi during startup transients. This requires that such a device be very strong mechanically. Fortunately, such rugged units are available commercially, although many of these units are definitely of inferior quality for even 10% accuracy in mass flow measurement. (An accuracy closer to 1% is usually required.) However, some experimenters accept some of these commercially available ΔP measuring devices, reporting them as adequately reliable and accurate (about 1% in mass flow) after a suitable "break-in" period of operation. Such break-in consists of exposing the unit to high rapidly-imposed differential pressures in both the upstream and downstream direction. It appears, therefore, that obtaining a 1% accuracy from existing commercial units would be largely fortuitous, and an accuracy of 10% would be more likely.

---

*Similar limitations hold for a subsonic nozzle.

Sonic nozzles having inlet radii about equal to throat radii are employed to a lesser extent than are the sharp-edged orifices discussed above. That these latter units simplify the mass flow rate measurement problem can be seen from the following, where the flow is given by:

$$\dot{m} = C \frac{P_1}{\sqrt{T}}, \quad P_2 \leq P^*$$

Thus the need for precise ΔP, where $\Delta P = P_2 - P_1$, measurements is eliminated because it is sufficient merely to monitor the downstream pressure P^*. (For air, $P^* \approx 1/2P$.)

Sonic nozzles are capable of 1% accuracy of mass flow measurement when calibrated properly. A similar degree of accuracy may be expected from uncalibrated nozzles when due account is taken of Reynolds number effects, downstream pressure effects, and particularly those effects due to compressibility (deviation from perfect gas behavior). Failure to consider the latter factor can result in measurement errors as high as 8% in systems having total pressures of 3000 psi and a total temperature of 70°F.

The principal disadvantage of the sonic system of measurement is the high loss in total pressure. Since virtually all of the pressure drop to the throat is lost, half or more of the supply pressure is also lost. In high pressure systems, such loss can constitute an intolerable waste.

Supersonic nozzles require the same measurements and have the same degree of accuracy as sonic nozzles. Their major advantage over sonic nozzles lies in their low loss of pressure. A slight complication arises from the fact that it is necessary to monitor the downstream pressure just slightly behind (downstream) of the throat if a low loss of pressure is to be realized. In operation, the supersonic flow in the divergent section "shocks" down to subsonic flow due to the imposed high back pressure. The gas then diffuses subsonically. This result in the recovery of a large portion of the dynamic head that existed just downstream of the shock wave.

Higher downstream pressures divert the shock wave upstream and vice versa. If the wave is driven upstream of the monitoring downstream pressure tap, it cannot be assured that the throat is running sonic. Therefore, this tap must extend into the divergent section just far enough to allow reliable determination that the local pressure is less than the critical pressure.

Supersonic units have been operated successfully at above 2000 psi supply pressures and 7% loss in total pressure. Supersonic nozzles with variable throats (but without the monitoring tap) are available commercially. One user (Ref. 9.1.1.1) reports good functioning of the nozzle for flow control, but has experienced some difficulties with the position readout used to calculate throat size.

9.1.2 Enthalpy Calculation Methods

Two methods of calculating stream enthalpy are commonly employed in designing and testing arc heater installations. These methods are: an energy balance method; and a compressible flow method.

The energy balance method commonly includes measuring the terminal voltage and arc current to measure power, although in some cases a wattmeter is used. (Some investigators attribute difficulties with wattmeter readings to the voltage wave-form.) Additional data taken include cooling water flow rate and temperature rise. Unless appropriate shielding precautions are taken, the thermocouples immersed in the cooling water are quite susceptible to stray pick-up from the magnetic field common to arc heater operation. At best, the energy balance method is probably accurate to only a few percent.

The "compressible flow" method of calculating stream enthalpy assumes an isentropic flow to sonic conditions at the nozzle throat. Real gas effects are considered, but local departure from the thermodynamic equilibrium is not considered. The equation employed is usually written as:

$$h = C\ T_c^{1.25} \left(\frac{P_h M_c}{P_c M_h} \right)^{2.5*}$$

As is suggested by the above equation, the throat area is not used directly but is effectively determined by a cold flow run. For arc heaters known to be free of swirl at the nozzle throat, an accuracy of a few percent would be expected from this technique. It can be shown that even a few degrees of swirl can cause the calculated enthalpy to be high by an appreciable amount. Unless it is known that the effluent is swirl free, the compressible flow method of calculating stream enthalpy is not recommended for use.

*Theoretical development, assuming c_p constant, leads to $h \sim p^2$. Curve fitting for variable c_p leads to $h \sim p^{2.5}$.

9.1.3 Radiation Effects

The division of heat transfer to the vessel walls between connections and radiation is of prime importance to the designer of arc heaters. Unfortunately, however, good data on this subject is not presently available. Work along these lines is currently under way at two locations at least, with the objective of determining the radiative component of such division. When forthcoming, such data will be of considerable value to designers and users in the arc heater field.

9.2 Throat Heat Flux and Total Pressure Loss Calculations

9.2.1 Primary Calculations

Some investigators have suggested that the nozzle throat heat flux problem could be reduced by adding a considerable portion of the total energy by means of heating a supersonic stream. Although it is recognized that this would impose an increase in arc heater operating pressure, the severity of this requirement is frequently not appreciated. The following paragraphs discuss a case for the Mach 11, 166,000 ft test condition, pointing out the severe pressure requirement on the are heater, as well as the extent of the hoped-for reduction in nozzle throat heat flux.

Consider a representative case of supersonic heating for a constant pressure heat addition. While there are processes which result in a smaller total pressure loss, generally these are more restricted in the amount of heat that may be added prior to reaching Mach 1. Consequently, such processes require a second throat -- which is to be avoided if the proposed advantages of supersonic heating are to be realized.

For simplicity in calculating the pressure drop, consider a perfect gas having constant specific heats and constant isentropic exponent. Although real gas effects are noticeable in the range of interest, the end results for an ideal gas are expected to be conclusive.

To review the process, refer to Fig. 9.2.1.1. Air is heated in an arc heater to total conditions corresponding to point 1. (Since flow speeds in conventional arc heaters are small compared with acoustic speed, the static and total conditions are essentially equal.) The gas is then expanded isentropically to static state 2. Next, it is heated at constant pressure to static state 3, having total conditions corresponding to 4. From 3 the gas is expanded isentropically to 5, with static conditions corresponding to the selected test altitude. At 5 the gas has total conditions per point 4, which corresponds to a given free-stream speed for point 5.

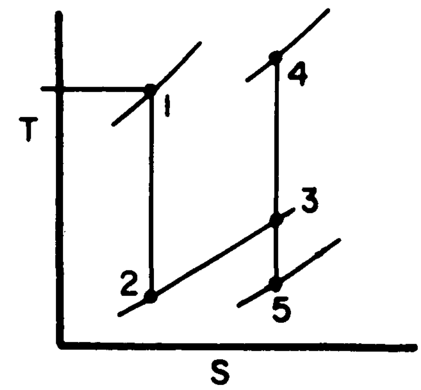

Figure 9.2.1.1

Clearly, then, the test altitude determines the state 5, and the combination of test altitude and test speed determines the total conditions, point 4. Required test conditions may be reached by an infinite number of supersonic constant pressure heating processes, each with a uniquely required state 1. By specifying a state property at 2, with the amount of heat added from 2 to 3 the process is fixed. This may be done conveniently by specifying the ratio of kinetic energy to total energy at 2, and the ratio of the energy added from 2 to 3 to the total energy at 3. For a perfect gas, the specification of the static to total energy is equivalent to specifying the same ratio of static to total temperature.

The conditions at point 2 are determined by the usual isentropic relations.

$$\frac{T_2}{T_1} = \frac{h_2}{h_1} = \alpha$$

$$\frac{P_2}{P_1} = \left(\frac{T_2}{T_1}\right)^{\frac{k}{k-1}} = \alpha^{\varphi}, \quad \varphi = \frac{k}{k-1}$$

State 3 may be related to 1 by

$$C_p \, T_2 + Q = C_p \, T_3$$

$$\frac{T_3}{T_1} = \frac{T_3}{T_2} \cdot \frac{T_2}{T_1} = \left(1 + \frac{Q}{C_p \, T_2}\right) \alpha = \alpha + \frac{Q}{C_p \, T_1}$$

$$= \alpha + \beta, \quad \beta = \frac{Q}{C_p \, T_1}$$

also

$$P_3 = P_2$$

$$\frac{P_3}{P_1} = \alpha^{\varphi}$$

It is convenient to have the entropy change from 2 to 3. Thus

$$\frac{\Delta S}{R} = \frac{C_p}{R} \ln \frac{T_3}{T_2} = \varphi \ln \frac{T_3}{T_2} = \varphi \ln \frac{T_3/T_1}{T_2/T_1}$$

$$\frac{\Delta S}{R} = \varphi \ln (1 + \beta/\alpha)$$

The temperature at 4 is determined by means of the energy equation

$$C_p T_1 + Q = C_p T_4$$

$$\frac{T_4}{T_1} = 1 + \beta$$

The pressure is found by

$$\frac{P_4}{P_3} = \left(\frac{T_4}{T_3}\right)^{\varphi} = \left[\left(\frac{T_4}{T_1}\right) \div \left(\frac{T_3}{T_1}\right)\right]^{\varphi} = \left(\frac{1 + \beta}{\alpha + \beta}\right)^{\varphi}$$

$$\frac{P_4}{P_1} = \frac{P_4}{P_3} \cdot \frac{P_3}{P_1} = \left(\frac{1 + \beta}{\alpha + \beta}\right)^{\varphi} \alpha^{\varphi}$$

$$\frac{P_4}{P_1} = \left[\frac{1 + \beta}{1 + \beta/\alpha}\right]^{\varphi}$$

The last equation above is particularly significant. P_4/P_1 is the fraction of the total pressure remaining after heat addition.

To continue the example, consider a representative case:

$Z = 166{,}000$ ft
$M = 11$
$k = 1.30$
$\alpha = .5$
$\beta = 1$

The value of k is an approximate average value for air for the above conditions. The α = .5 corresponds to a Mach number of 2.6 at point 2, and β = 1 corresponds to adding one-half of the total stream energy at the test section via constant pressure supersonic heating. From these values we obtain

$$\varphi = \frac{k}{k - 1} = \frac{1.30}{1.30 - 1} = 4.33$$

$$\frac{P_4}{P_1} = \left(\frac{1 + \beta}{1 + \beta/\alpha}\right)^{\varphi} = \left(\frac{1 + 1}{1 + \frac{1}{.5}}\right)^{4.33} = .667^{4.33} = 0.1728$$

Thus an intolerable loss of 83% of the total pressure has been incurred.

The pressure at 5 (see footnote 1) is

$$P_5 = 7.31 \times 10^{-4} \text{ atm}$$

The pressure at 4 may be obtained by

$$\frac{P_5}{P_4} = \left(1 + \frac{k - 1}{2} M^2\right)^{\frac{k}{1 - k}} \Bigg| \begin{array}{l} P_4 = 7.31 \times 10^{-4} \\ M = 11 \\ k = 1.30 \end{array}$$

$$P_4 = 260 \text{ atm}$$

From the above

$$\frac{P_4}{P_1} = .1728$$

$$P_1 = \frac{P_4}{.1728} = \frac{260}{.1728} = 1503 \text{ atm}$$

---

1. "U.S. Standard Atmosphere, 1962." Prepared under sponsorship of NASA, USAF and USWB, Washington D.C., Dec. 1962.

The pressure in the heating section is given by

$$\frac{P_3}{P_1} = \alpha^{\varphi}$$

$$P_3 = (.5)^{4.33}\ 1503$$

$$P_3 = 74.8 \text{ atm}$$

The temperature at 5 (see footnote 1) is

$$T_5 = 487^{o}R$$

Using the usual isentropic relations between points 5 and 4 we obtain

$$\frac{T_4}{T_5} = \left(1 + \frac{k-1}{2} M^2\right)\Bigg|_{\substack{T_5 = 487 \\ M = 11 \\ k = 1.30}}$$

$$T_4 = 9326^{o}R$$

It has been shown that

$$\frac{T_4}{T_1} = 1 + \beta$$

Therefore

$$T_1 = \frac{T_4}{1+\beta} = \frac{9326}{1+1} = 4663^{o}R$$

Also

$$\frac{T_2}{T_1} = \alpha$$

$$T_2 = \alpha T_1 = (.5)(4663) = 2332^{o}R$$

---

1. "U.S. Standard Atmosphere, 1962." Prepared under sponsorship of NASA, USAF and USWB, Washington D.C., Dec. 1962.

Further

$$\frac{T_3}{T_1} = \alpha + \beta$$

$$T_3 = (\alpha + \beta) T_1 = (.5 + 1)(4663)$$

$$T_3 = 6994^{\circ}R$$

Since

$$\frac{S_3}{R} = \frac{S_4}{R} = \frac{S_5}{R}$$

Also (see footnote 1) $\frac{S_5}{R} = 30.80$

Evaluating the equation for $\frac{\Delta S}{R}$ gives

$$\frac{\Delta S}{R} = \varphi \ln (1 + \beta / \alpha)$$

$$= 4.33 \ln \left(1 + \frac{1}{.5}\right)$$

$$\frac{\Delta S}{R} = 4.76$$

Therefore

$$\frac{S_1}{R} = \frac{S_2}{R} = \frac{S_5}{R} - \frac{\Delta S}{R} = 30.80 - 4.76 = 26.04$$

Figure 9.2.1.2 summarizes these findings on a temperature-entropy plot.

An alternate process employing, say, an arc heater, would heat the gas with negligible speed and at constant pressure directly to state 4. Subsequently the air would be expanded to the test section condition according to state 5. Here the nozzle throat heat fluxes are compared for the two processes.

1. Moeckel, W. E. and Weston, K. C., "Composition and Thermodynamic Properties of Air in Chemical Equilibrium", NACA TN4265, April 1958.

For such comparison, an equation (see footnote 1) due to Bartz may be employed; e.g.

$$h_g = \left[\frac{.026}{D^{*.2}} \left(\frac{\mu^{.2} C_p}{P_r^{.6}} \right)_o \left(\frac{P_c\, g}{C*} \right)^{.8} \left(\frac{D^*}{r_c} \right)^{.1} \right] \left(\frac{A^*}{A} \right)^{.9} \sigma$$

with

h_g - gas side heat transfer coefficient (BTU/In^2 Sec ^{o}R)

D^* - throat diameter (In)

μ - viscosity at total condition (#/In Sec)

C_p - constant pressure specific heat at total condition (BTU/# ^{o}R)

Pr - Prandtl number at total conditions

P_c - chamber (total) pressure (#/In^2)

g_c - gravitational constant (Ft/Sec^2)

$C*$ - characteristic velocity (Ft/Sec)

r_c - nozzle throat radius of curvature (In)

A - local flow area (In^2)

A^* - throat flow area (In^2)

σ - dimensionless factor accounting for variations of ρ and μ values across boundary layer.

From a paper by Lewis and Horn[2] it can be shown that $\frac{P_c\, g}{C*} = \frac{\dot{m}}{A^*}$ where m is the mass flow in slugs/sec.

In using the Bartz equation it is desirable to employ real air properties as far as is convenient. However, where data is not readily available a perfect gas with k = 1.30 has been used. The following values and their sources were utilized for the supersonic case:

---

1. Bartz, D. R. "A Simple Equation for the Rapid Estimation of Rocket Nozzle Convective Heat Transfer Coefficients" Jet Propulsion, January 1957.
2. Lewis, H. F. and Horn, D. D., "Some Considerations in the Design of Water-Cooled Nozzle Throat Sections for High Temperature, High Pressure Operation" AEDC-TDR-64-51, April 1964.

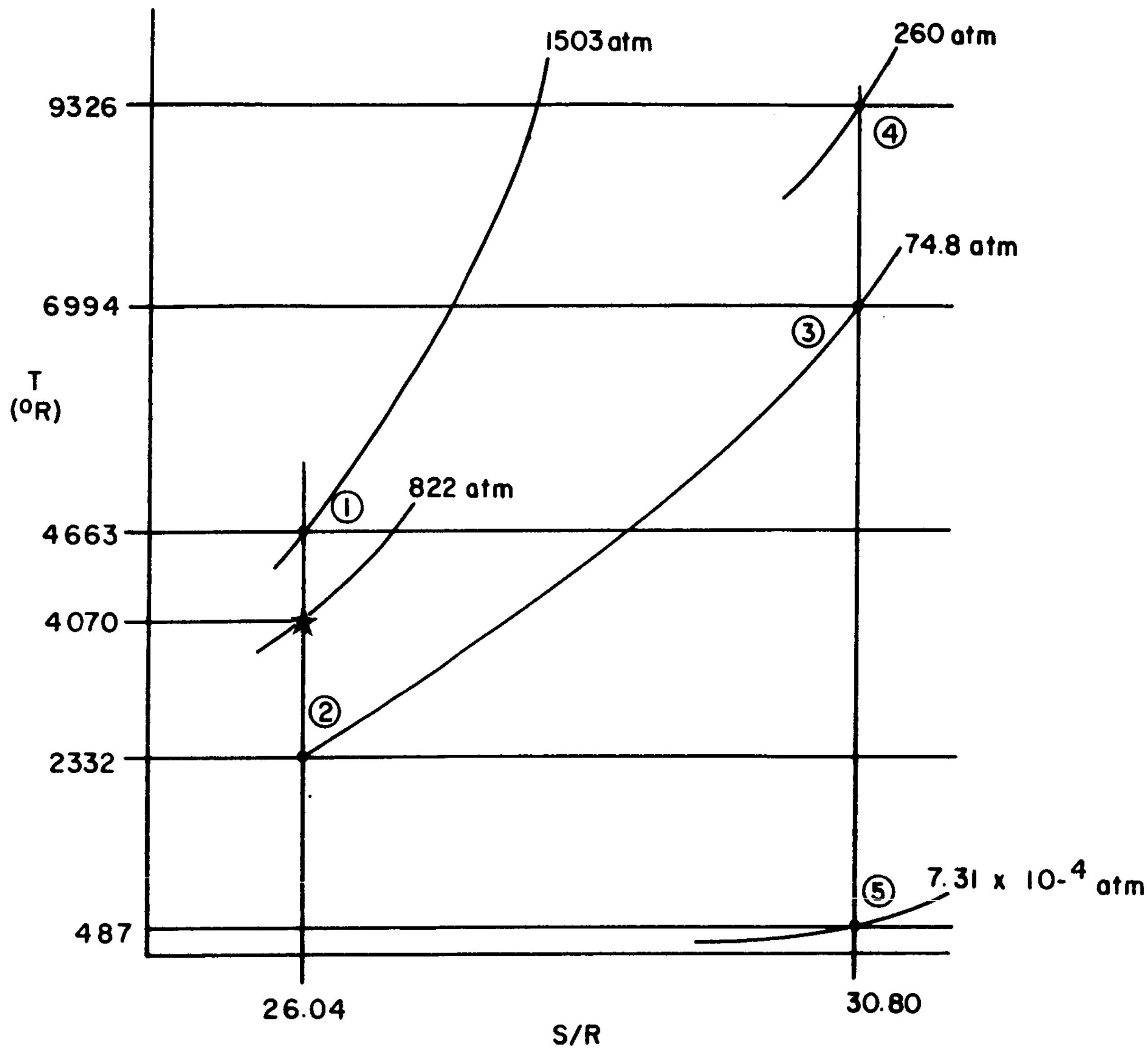

Figure 9.2.1.2 Supersonic Heating with α = .5, β = 1, k = 1.3

σ = 1.38 read from Bartz[1]

$\frac{A}{A^*}$ = 1.000 throat condition

$\frac{D^*}{r_c}$ = 0.400 assumed as representative

$\frac{P_c\, g}{C_*} = \frac{\dot{m}}{A^*}$ = 168.3 from 20#/sec flow required in M = 11 and 166,000 ft condition and A* calculation in section 9.2.2

μ = 4.5×10^{-6} lb/in sec., see section 9.2.3

C_p = 0.315 Btu/#°R from Hansen[2] with $Z \approx 1$, $C_p \approx C_p$ at 100 atm and R = 0.0686 Btu/#°R

Pr = .70 from ref. 5. This appears to be a representative value, although data do not extend to these pressures.

D^* = .388 in, from A* calculation, section 9.2.2

The above gives

$$h_g = .080 \text{ Btu/in}^2 \text{ Sec } {}^oR = 4.15 \times 10^3 \text{ Btu/hr ft}^2 \, {}^oR$$

The free stream temperature at the throat may be estimated by

$$\frac{T^*}{T_0} = \frac{2}{k+1} = \frac{2}{2.30} = .870$$

$$T^* = .870 \times 2595 = 2260^oK$$

Assuming a nozzle gas side wall temperature of 600°K

$$\Delta T = 1660^oK = 2990^oR$$

This gives a heat flux

$$\varphi = h_g \Delta T = (4.15 \times 10^3)(2.99 \times 10^3)$$

$$\varphi = 12.42 \times 10^6 \text{ BTU/hr ft}^2$$

---

1. Bartz, op. cit.
2. Hansen, C. F., "Approximations for the Thermodynamic and Transport Properties of High-Temperature Air", NASA R-50, 1959

For comparison, consider the constant pressure heating shown in Fig. 9.2.1.3. Values used in the Bartz equation are:

$\sigma = 1.5$

$\frac{A}{A^*} = 1.000$

$\frac{D^*}{r_c} = .400$

$\frac{P_c\, g}{C_*} = \frac{\dot{m}}{A^*} = 19.38$

see Section 9.2.2 for calculation of A*

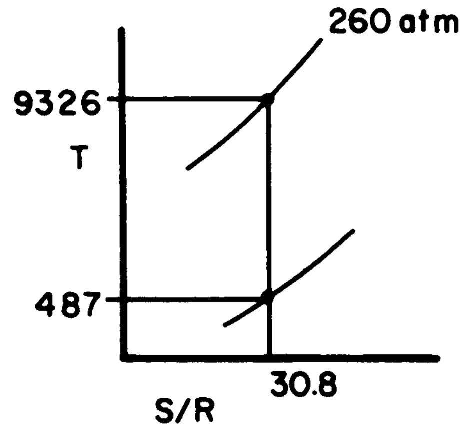

Figure 9.2.1.3

$\mu = 6.5 \times 10^6$ See Section 9.2.3

$C_p = .686$ from Hansen[1]

$Pr = .70$

$D^* = 1.240$ in (from A* calculation, Section 9.2.2)

These values give

$h_g = .0263\ \text{Btu/In}^2\ \text{Sec}\ {}^oR = 1.36 \times 10^3\ \text{Btu/hr ft}^2\ {}^oR$

Free stream temperature at the throat becomes

$T^* = .870\ T_0 = .870 \times 9326 = 8110^oR$

Taking $T_w = 600K = 1080R$

$\Delta T = 7030^oR$

This gives a heat flux

$\varphi = h\Delta T = (1.36 \times 10^3)(7030)$

$\varphi = 9.57 \times 10^6\ \text{BTU/ft}^2\ \text{hr}$

Note this is less than for the case of supersonic heating.

1. Hansen, C. F. op. cit.

From the above, it is obvious that:

(a) Supersonic heating imposes an extremely severe penalty on the system by requiring very high arc heater pressures.

(b) Supersonic heating will not provide a significant reduction in nozzle throat heat flux.

9.2.2 Calculation of A* values,

Supersonic Heating

Assuming a perfect gas, therefore:

$$\rho_1 = \frac{P_1}{R\,T_1} = \frac{1503 \times 2120}{53.3 \times 4663} = 12.83 \ \#/Ft^3$$

The isentropic relation for expansion to Mach 1 gives

$$\frac{\rho_2}{\rho_1} = \left(\frac{k+1}{2}\right)^{\frac{1}{1-k}} = \left(\frac{1.30+1}{2}\right)^{\frac{1}{1-1.30}}$$

$$\frac{\rho_2}{\rho_1} = .628$$

therefore

$$\rho_2 = .628\,\rho_1 = (.628)\,(12.83) = 8.06 \ \#/Ft^3$$

Also

$$\frac{T_2}{T_1} = \frac{2}{k+1} = \frac{2}{1.3+1} = .870$$

$$T_2 = .870\ T_1 = (.870)\,(4663) = 4050^{\circ}R$$

The acoustic speed becomes

$$a = \sqrt{kRT} = \sqrt{1.30 \times 1717 \times 4050}$$

$$a = 3010 \ ft/sec$$

From the one-dimensional continuity equation

$$\dot{m} = \rho \, u \, A = \rho^* u^* A^* = \rho_2 \, a \, A^*$$

$$A^* = \frac{\dot{m}}{\rho_2 a} = \frac{20}{8.06 \times 3010} = .824 \times 10^{-3} \text{ Ft}^2$$

$$A^* = .1188 \text{ In}^2 = \frac{\pi}{4} D^{*2}$$

$$D^* = \frac{4 \times .1188}{\pi} = .1513 = 0.388 \text{ in}$$

Negligible Speed Heating

Similarly, for the case of heating with negligible speed:

$$\rho_0 = \frac{P_0}{R \, T_0} = \frac{260 \times 2120}{53.3 \times 9326} = 1.110 \text{ \#/Ft}^3$$

$$\frac{\rho_1}{\rho_0} = .628$$

$$\rho_1 = (.628)(1.110) = .697 \text{ \#/Ft}^3$$

$$\frac{T_1}{T_0} = .870$$

$$T_1 = (.870)(9326) = 8110$$

$$a = \sqrt{1.3 \times 1717 \times 8110} = 4250 \text{ ft/sec}$$

$$A^* = \frac{20}{.697 \times 4250} = 6.75 \times 10^{-3}$$

$$A^* = .973 \text{ In}^2$$

$$D^* = \sqrt{\frac{4}{\pi} (.973)} = 1.240 \text{ in}$$

9.2.3 Viscosity Calculations

The viscosity may be calculated using reduced pressures and temperatures. Data for calculations include the source of ref. (9.2.3.1).

$P_c = 37.2$ atm

$T_c = 132.4K$

$\eta_c = .4 \times 10^{-6}$ # sec/ft^2 $= 1.048 \times 10^{-6}$ lb/in sec

For Stagnation Conditions

$$\left.\begin{array}{l} P = 1503 \text{ atm} \quad , P_r = 40.4 \\ T = 4663R = 2690K, \ T_r = 20.3 \end{array}\right\} \eta_r = \frac{\eta}{\eta_c} = 4.3$$

$\eta = 4.3 \times 1.05 \times 10^{-6} = 4.5 \times 10^{-6}$ lb/in sec

$$\left.\begin{array}{l} P = 260 \text{ atm}, \ P_r = 6.98 \\ T = 9326R = 5180K, \ T_r = 39.1 \end{array}\right\} \frac{\eta}{\eta_c} = 6.2$$

$\eta = 6.2 \times 1.05 \times 10^{-6} = 6.5 \times 10^{-6}$ lb/in sec

10. FIGURES

The following figures constitute Section 10 of this report.

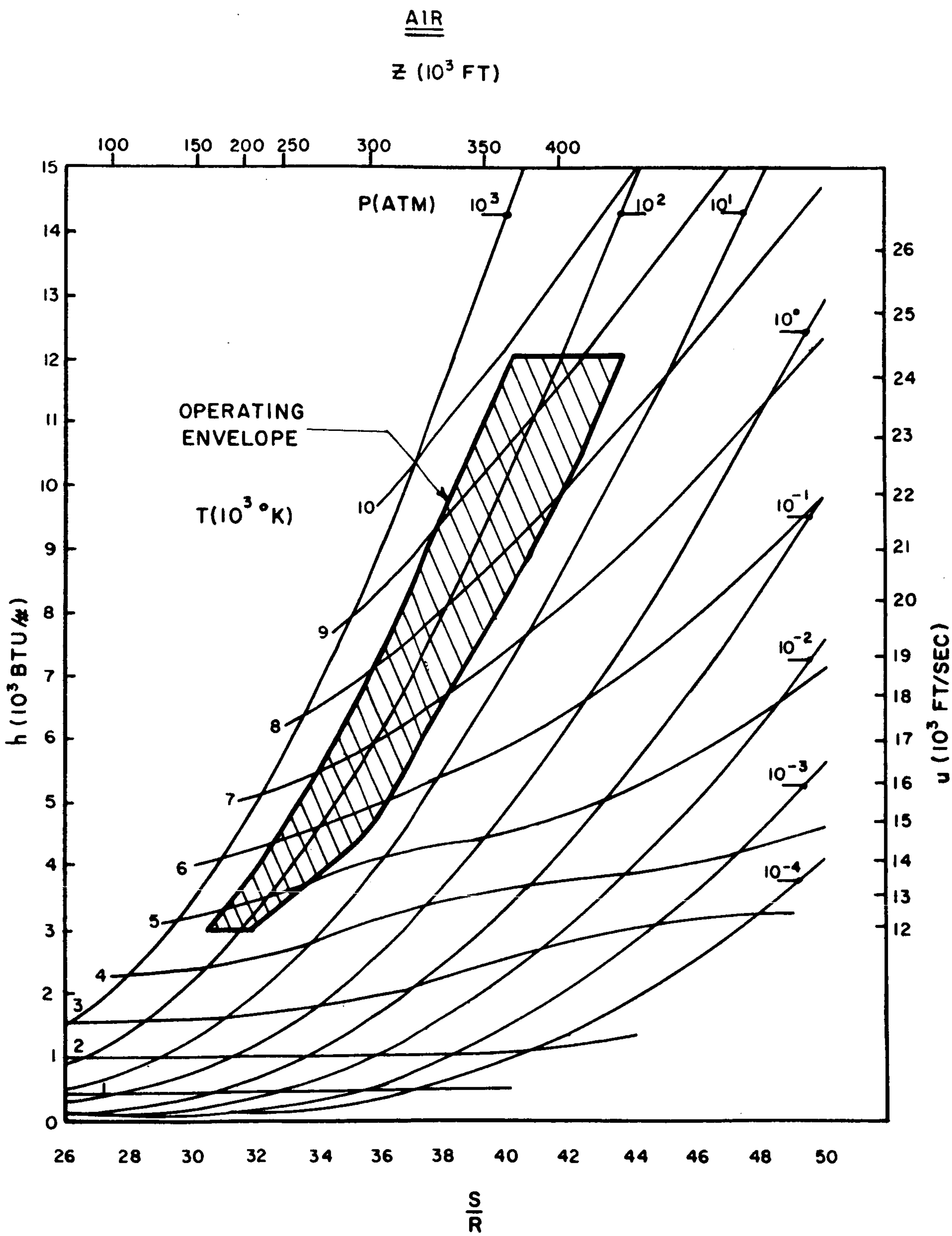

Figure 1.1-1 The Operating Envelope

PERFORMANCE ENVELOPE
FOR SIX FOOT DIAMETER
TEST SECTION

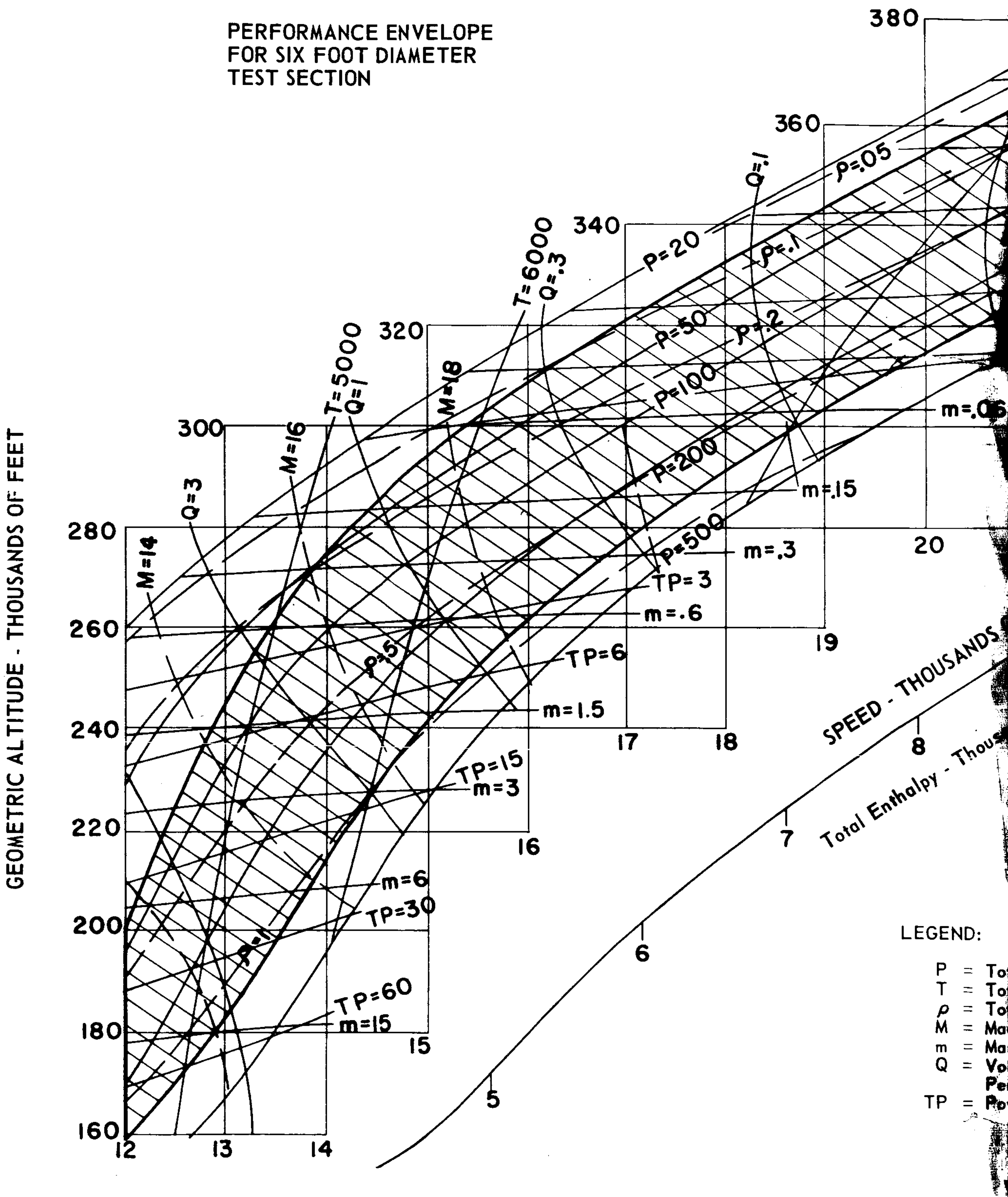

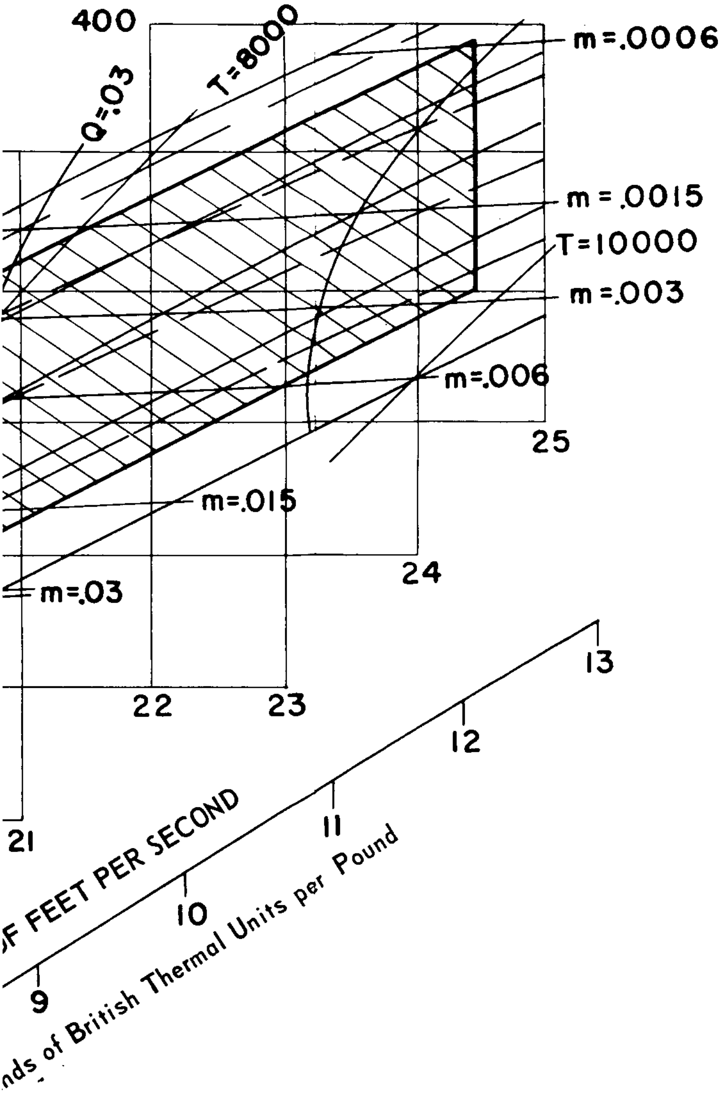

al Pressure, Atmospheres
al Temperature, Degrees Kelvin
tal Mass Density, Pounds Per Cubic Foot
ch Number
ss Flow Rate, Pounds Per Second
lume Flow Rate at Total Density, Cubic Feet
Second
wer, Megawatts

Figure 1.1-2

2

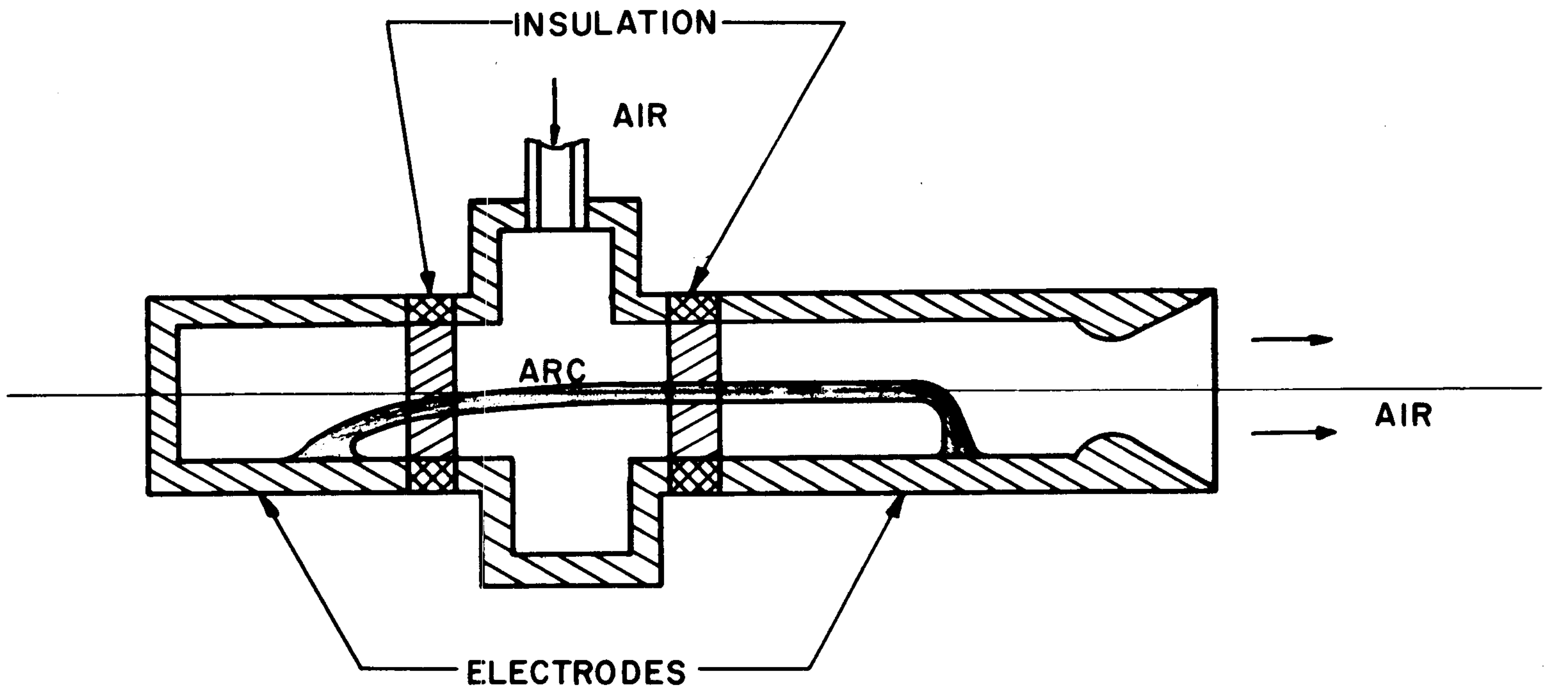

Figure 2.1.1.1-1 Axial Flow Arc Heater With Long Electrodes

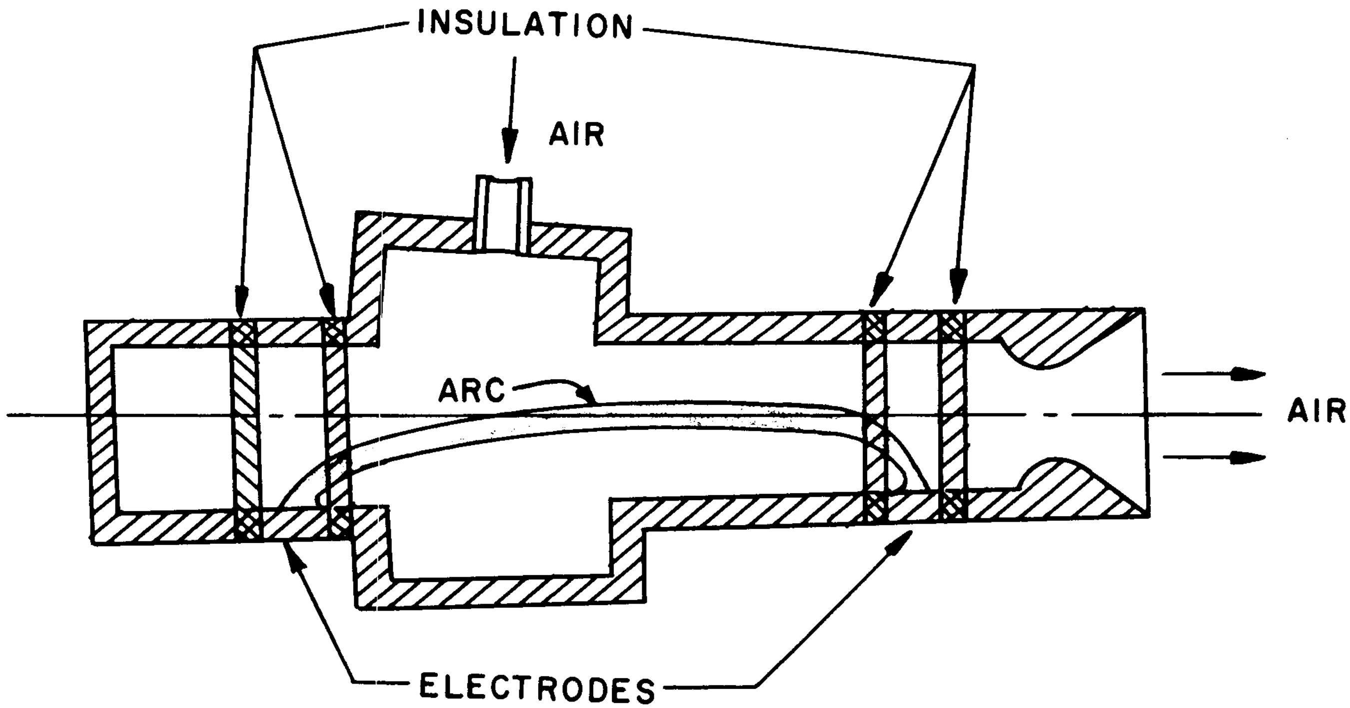

Figure 2.1.1.1-2 Axial Flow Arc Heater With Short Electrode

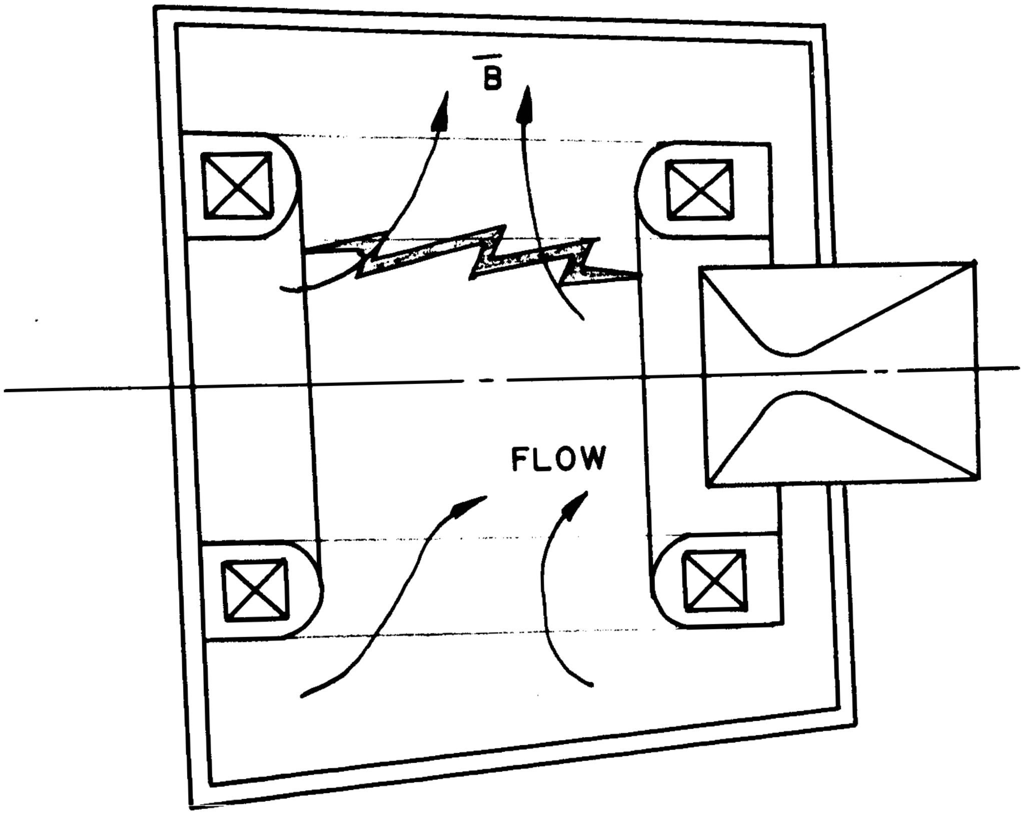

Figure 2.1.1.2-1 Cross Flow AC or DC Arc Heater

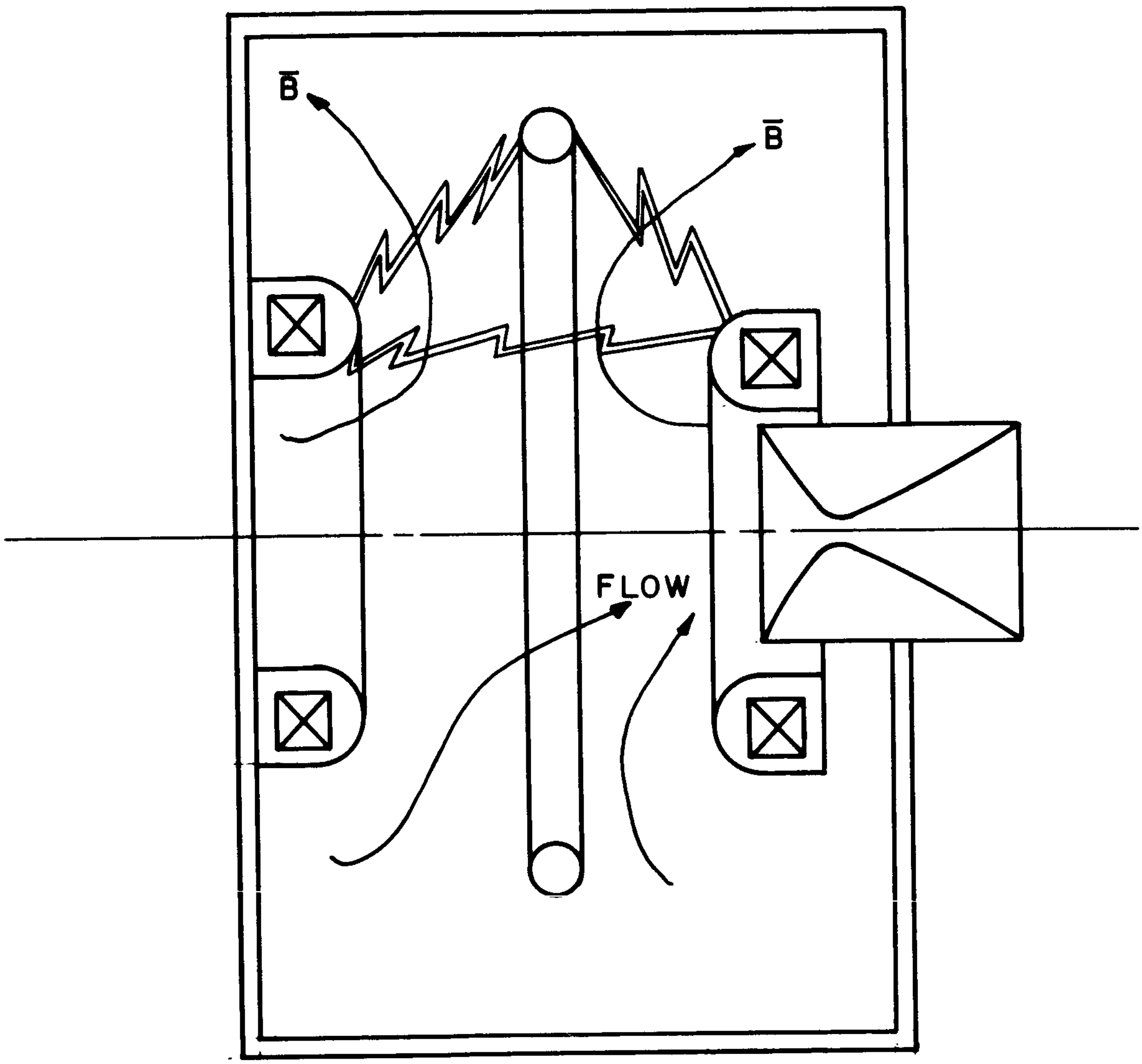

Figure 2.1.1.2-2 Three Phase, Three Electrode, Arc Heater

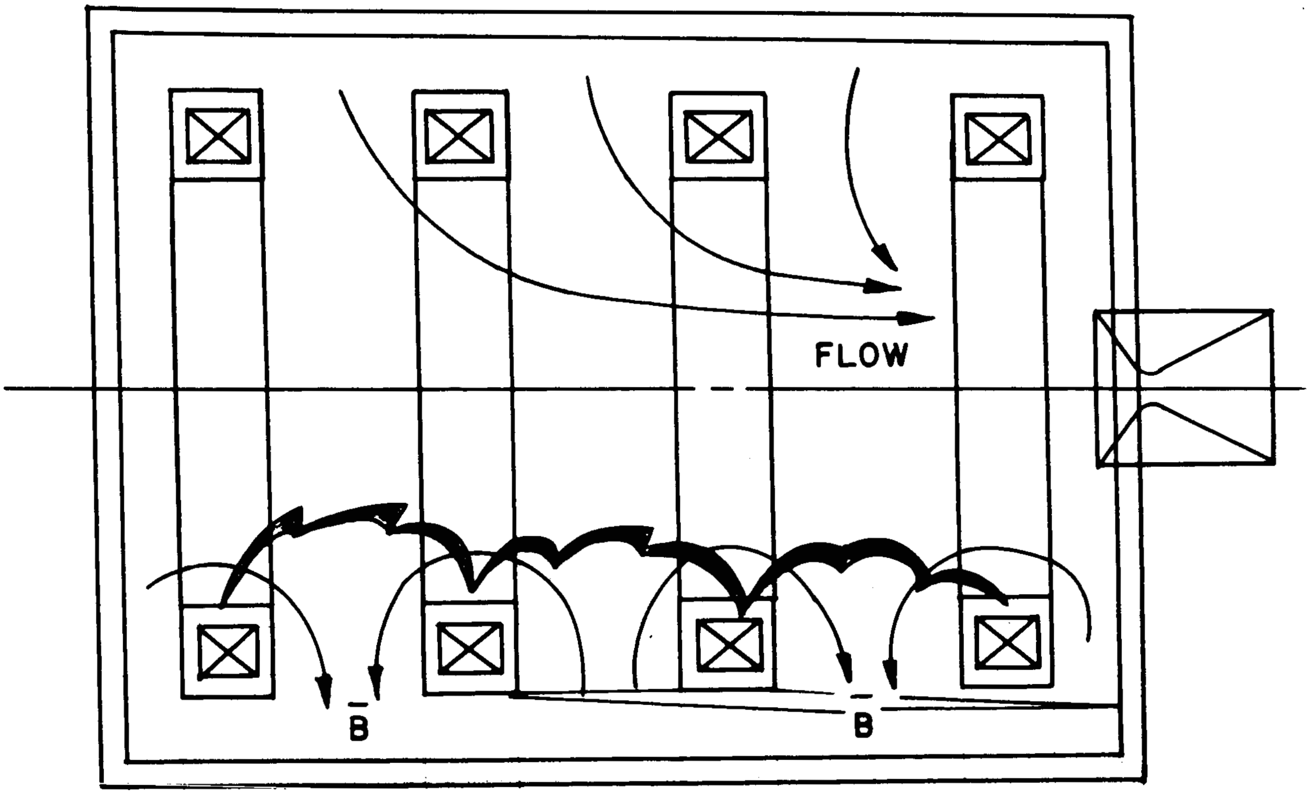

Figure 2.1.1.2-3 Three Phase, Four Electrode, Arc Heater

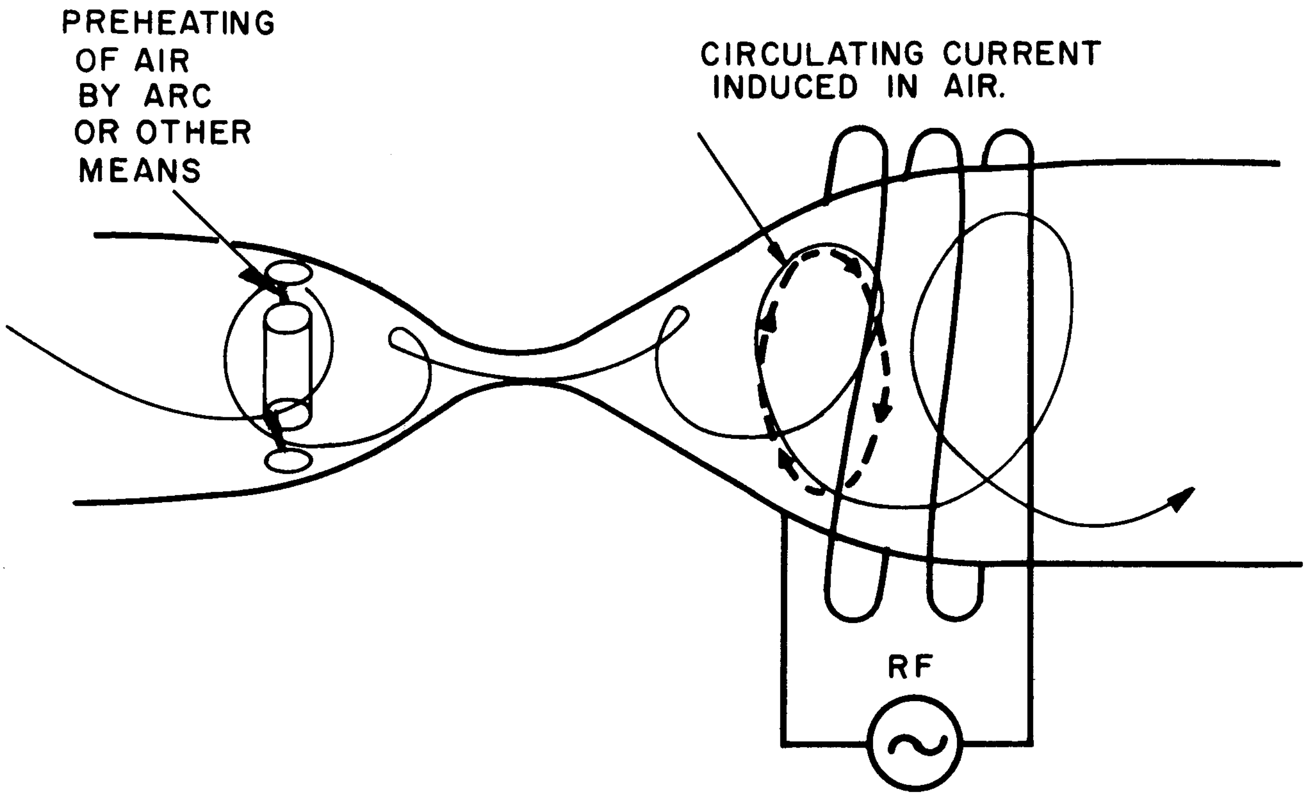

Figure 2.1.2-1 High Frequency Discharge (RF) Heater

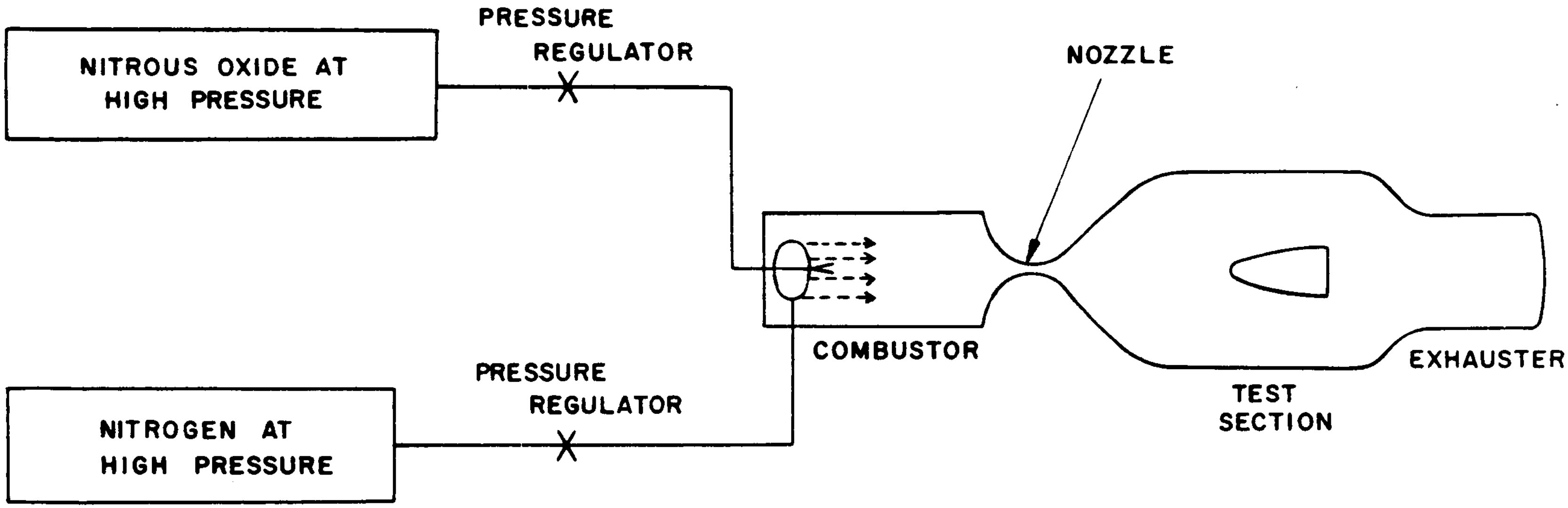

$$0.4NO + 0.6N_2 \longrightarrow 0.8N_2 + 0.2O_2 + Q$$

$$Q = 360\ BTU/\#$$

Figure 2.1.3-1 Nitrous Oxide Combustion System

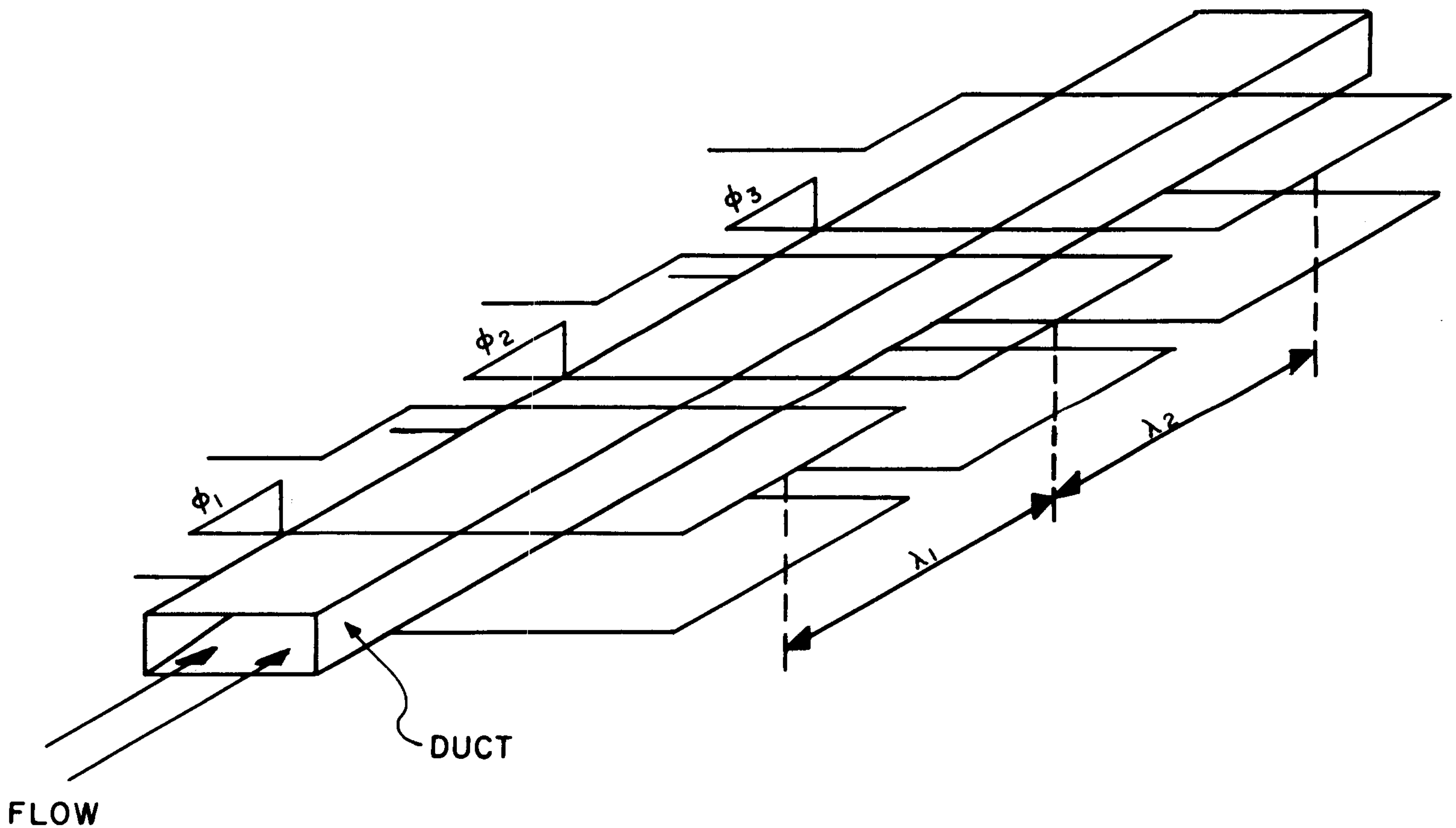

Figure 2.2.2-1 Traveling Wave Accelerator (AC MHD)

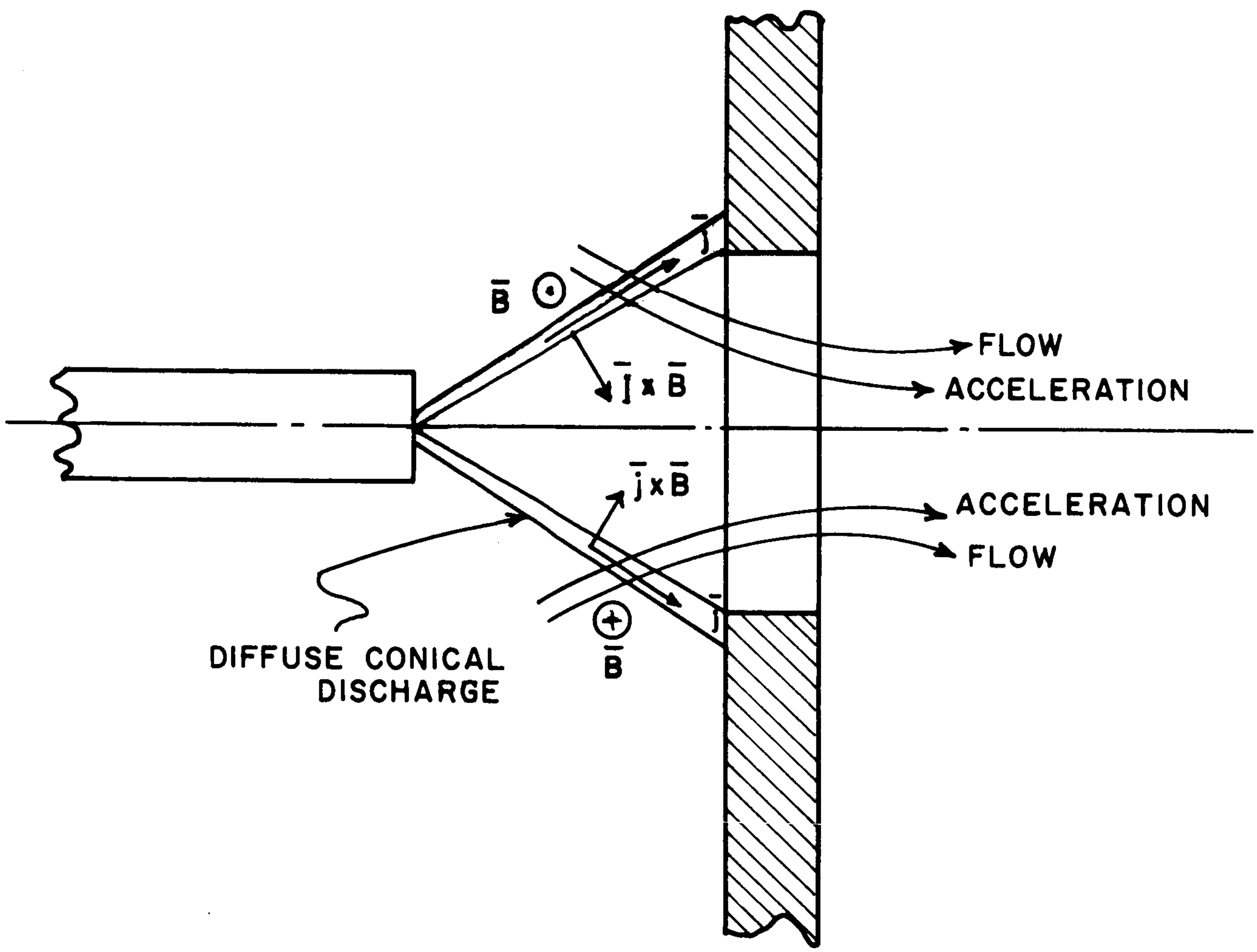

Figure 2.2.3-1 Self-Induced MHD Accelerator

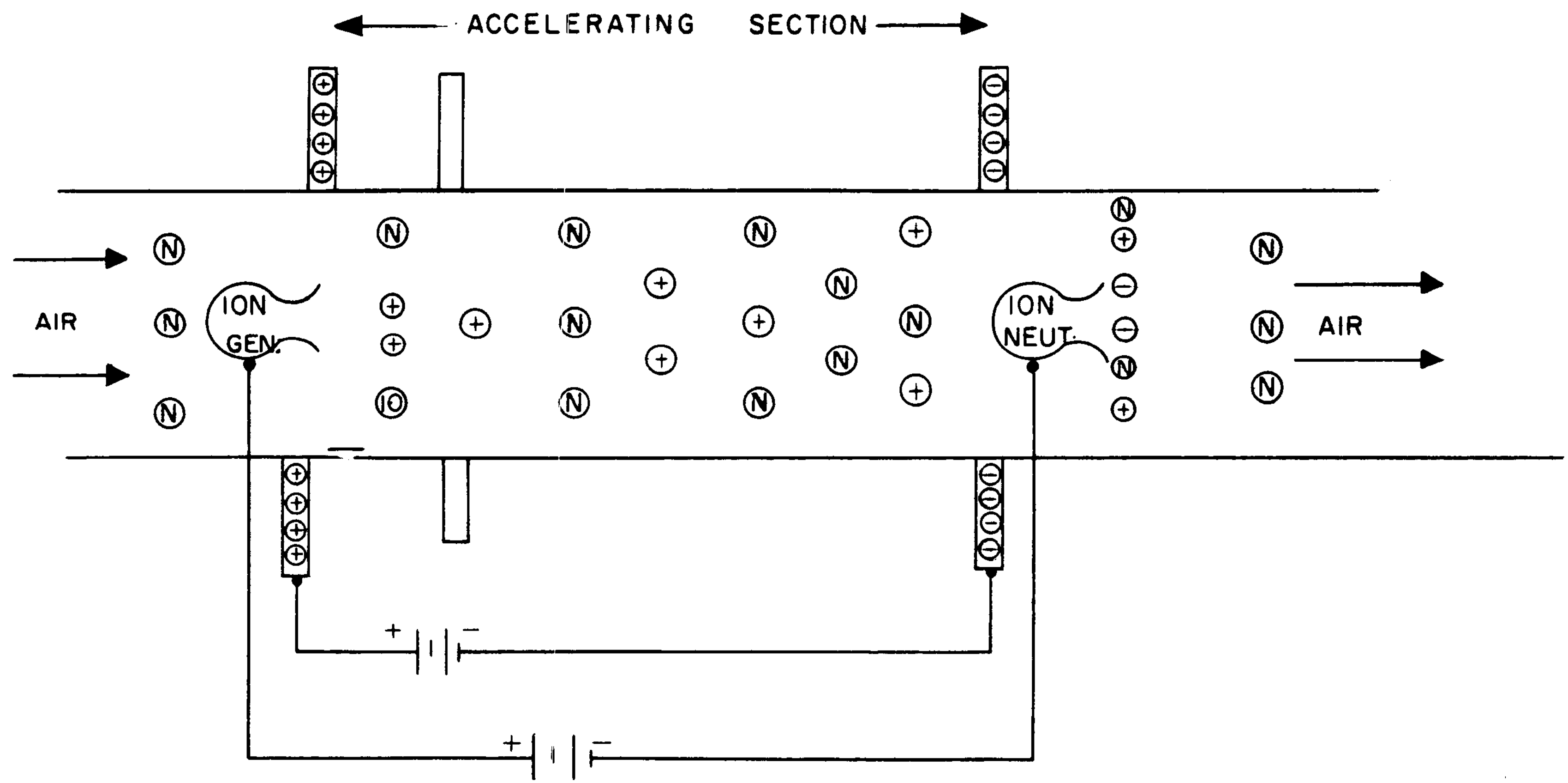

Figure 2.2.4-1 Electrostatic Accelerator

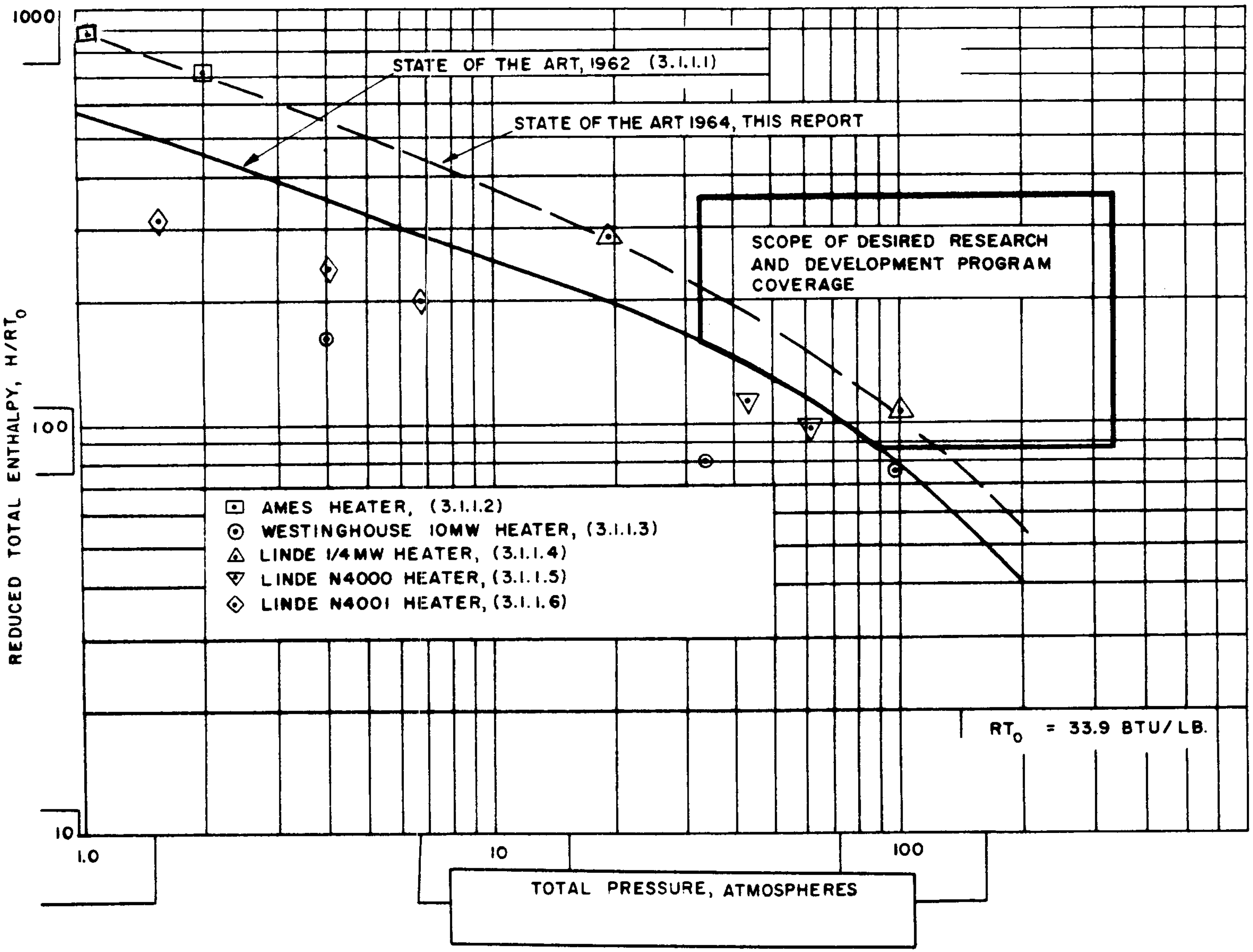

Figure 3.1.1-1 Present State of the Art

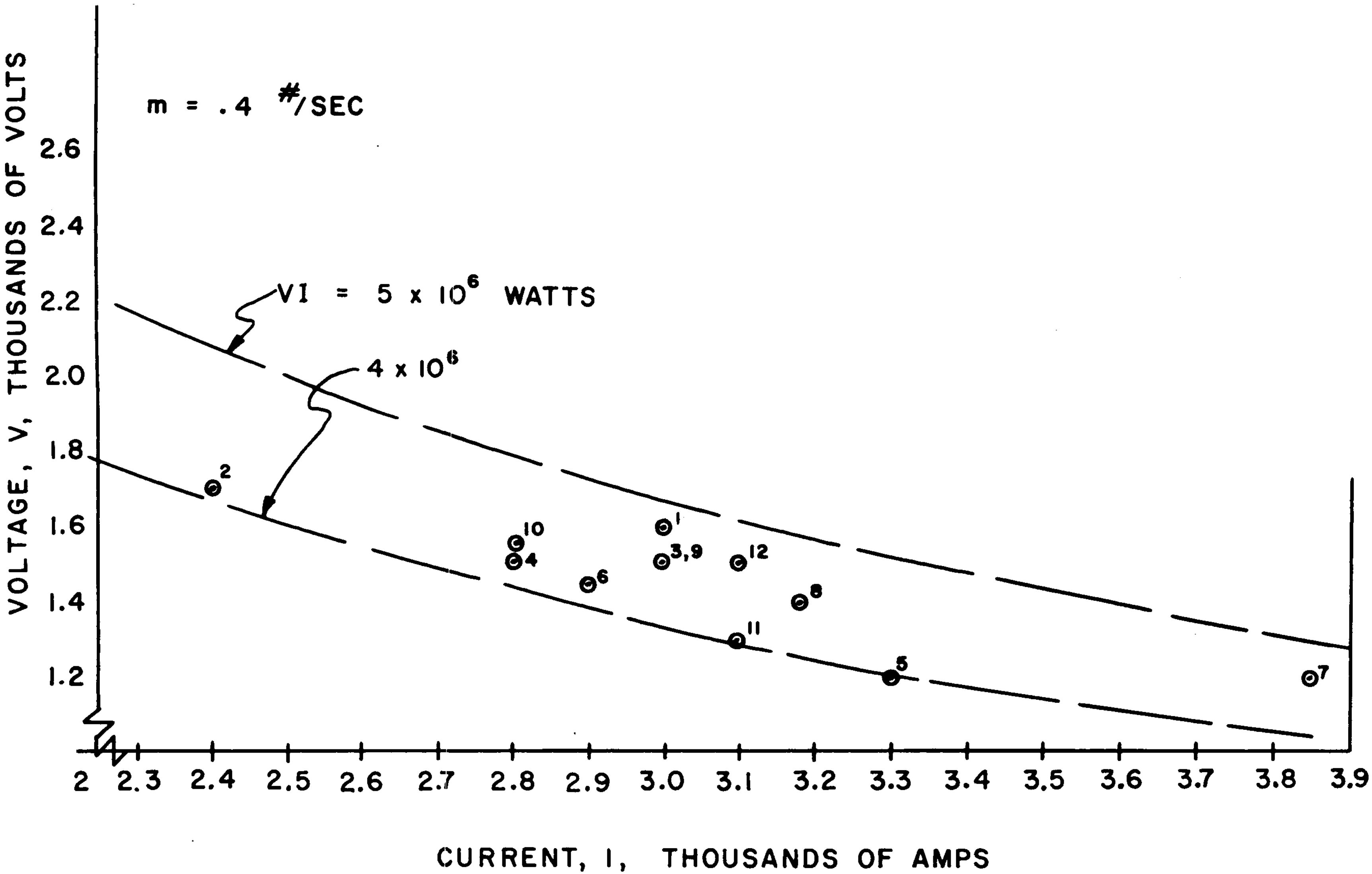

MARC 50 DATA SHOWING CONSTANT POWER CHARACTERISTICS

Figure 4.1.2-1 Typical Constant Power VI Curve

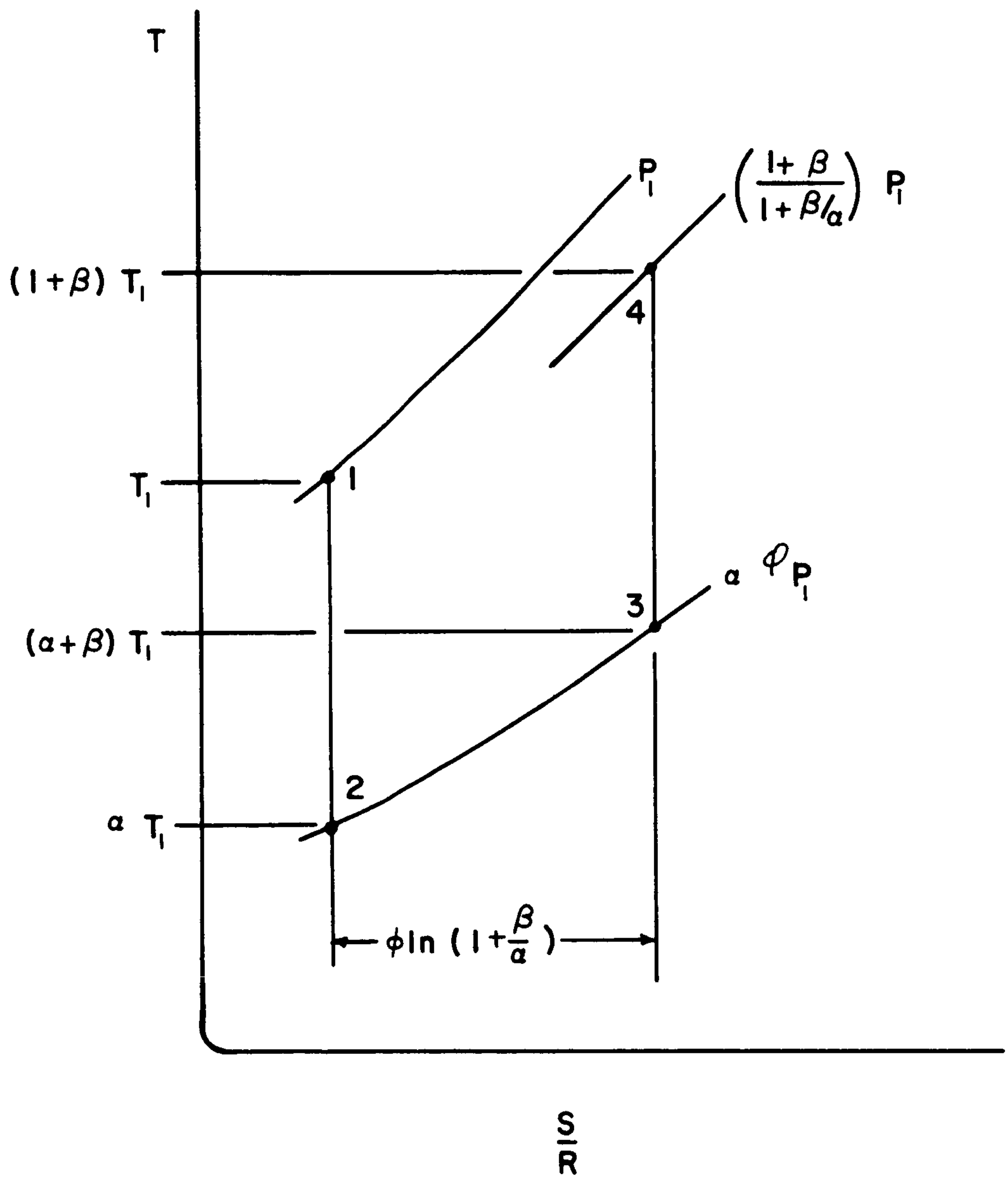

Figure 4.1.3-1 Supersonic Heating at Constant Pressure

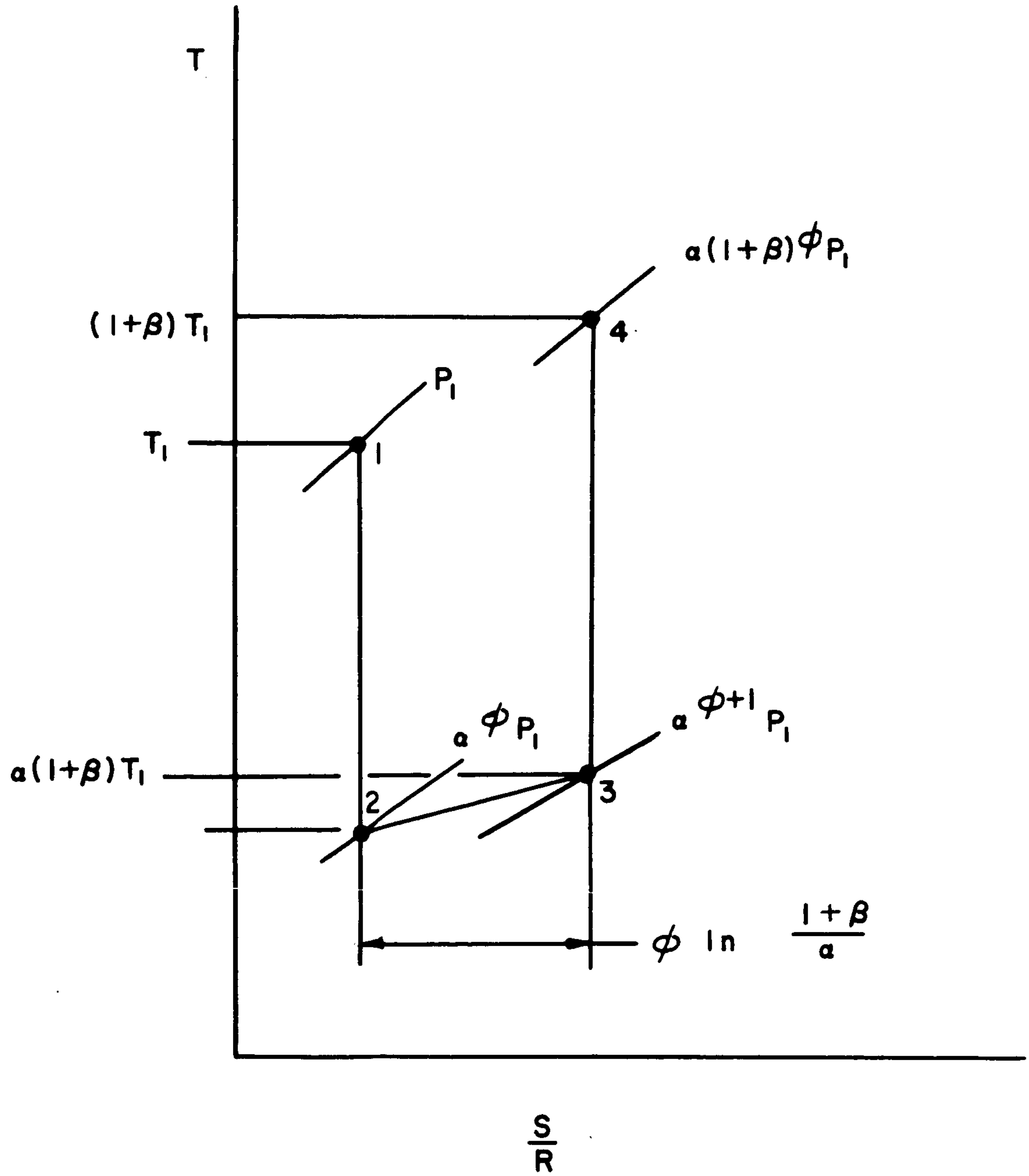

Figure 4.1.3-2 Supersonic Heating at Constant Mach Number

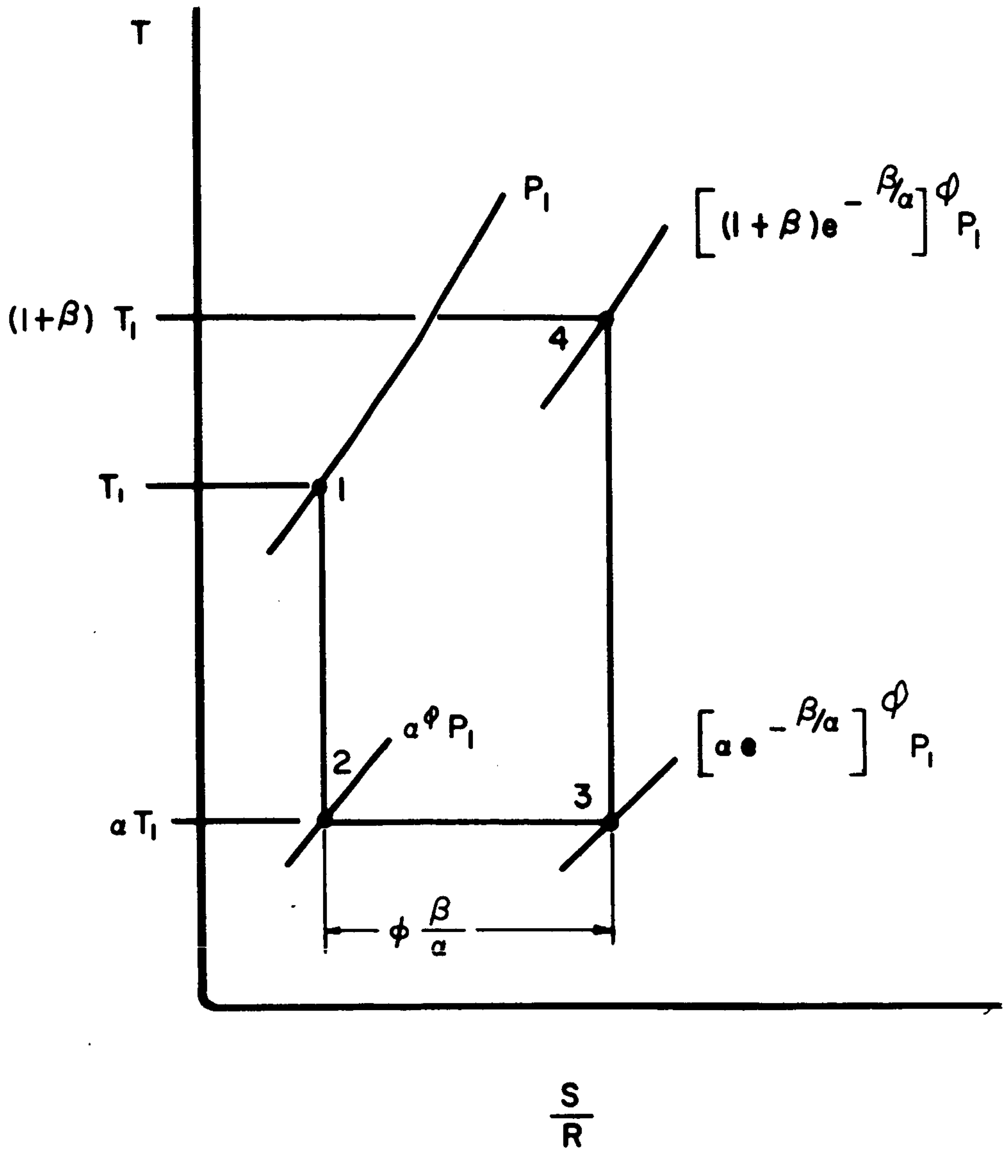

Figure 4.1.3-3 Supersonic Heating at Constant Temperature

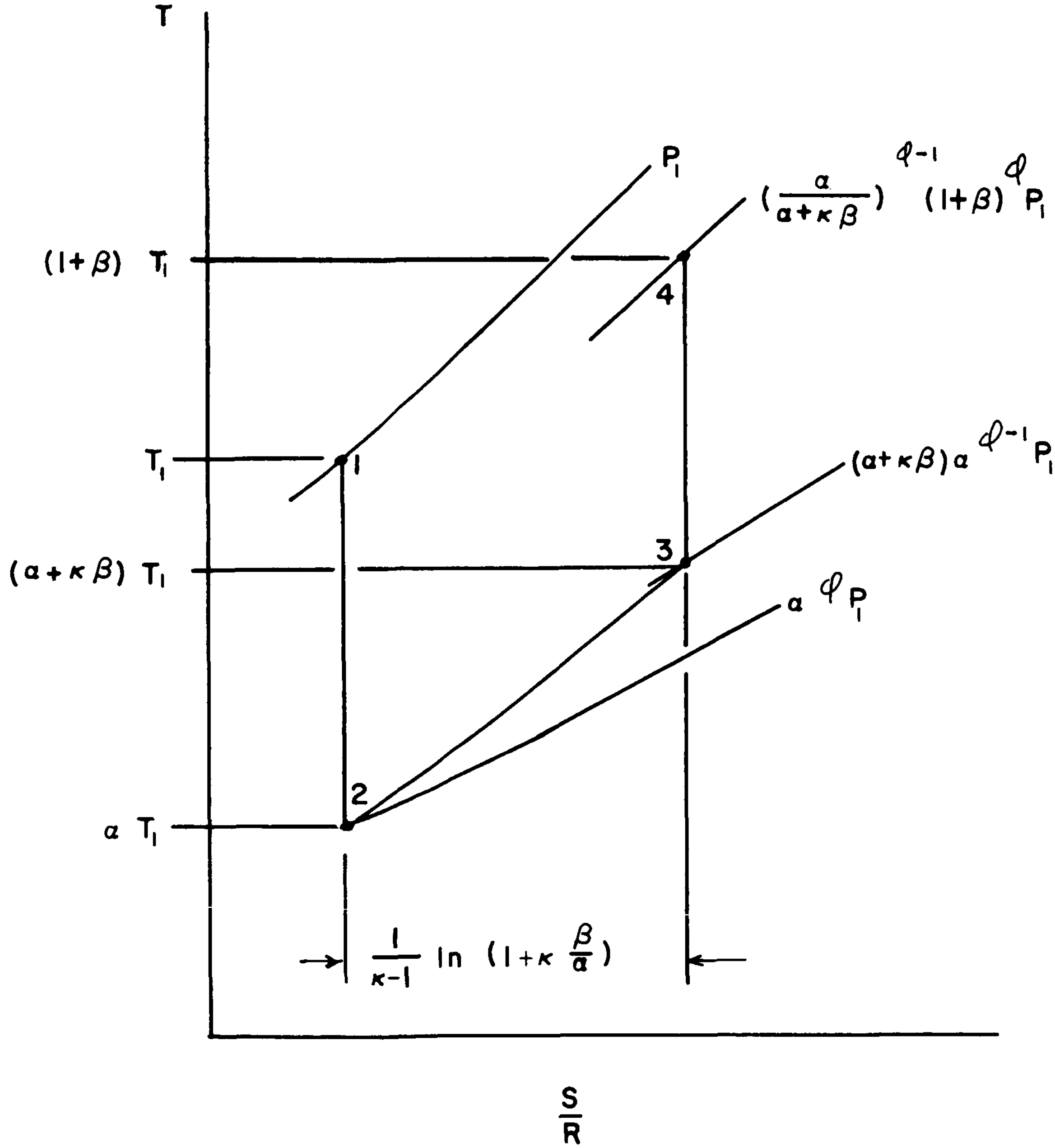

Figure 4.1.3-4 Supersonic Heating at Constant Density

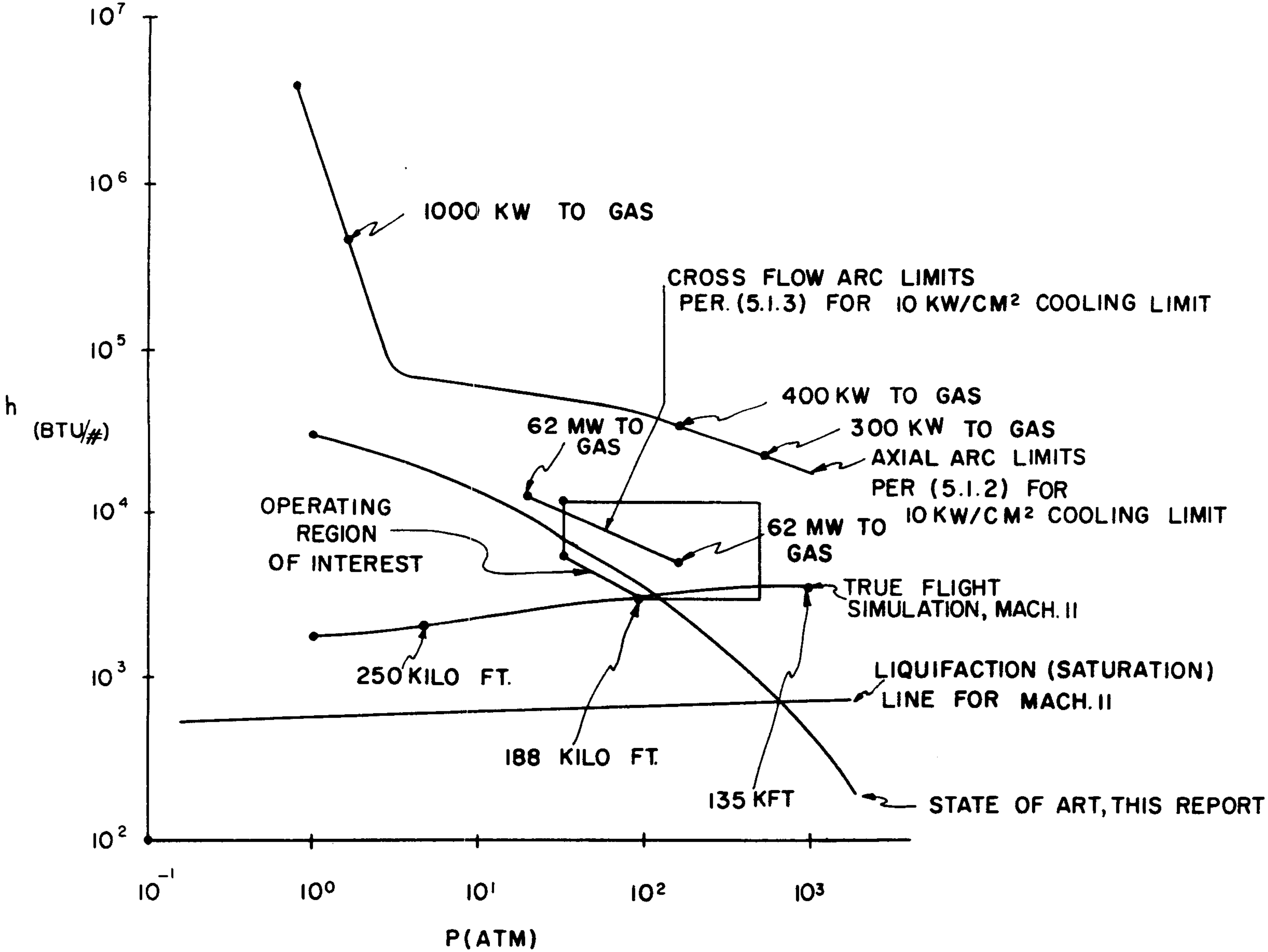

Figure 5.1-1 Preliminary Comparison of Cross & Axial Flow Arc Heaters

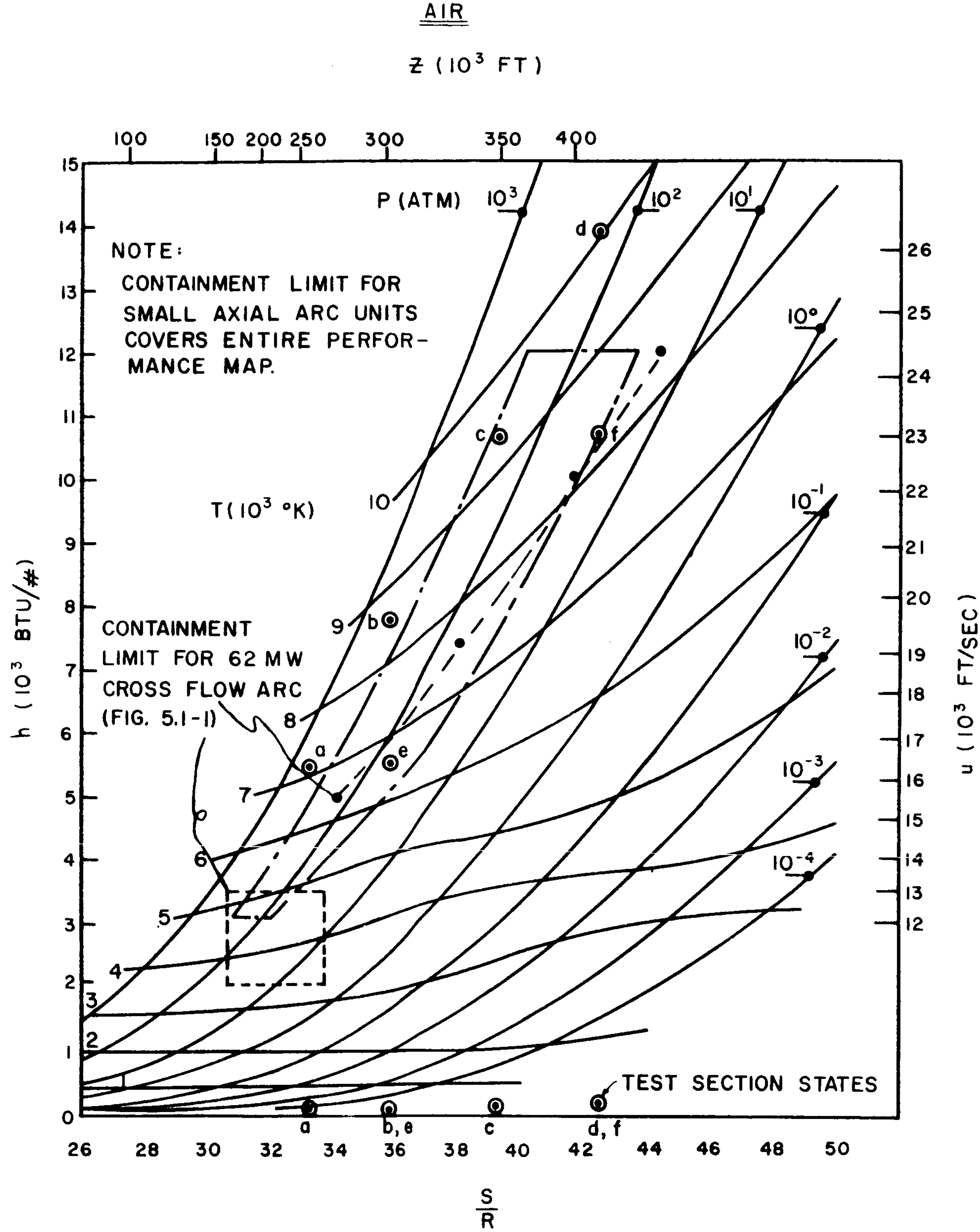

Figure 5.2-1 DC MHD Operating Points Investigated

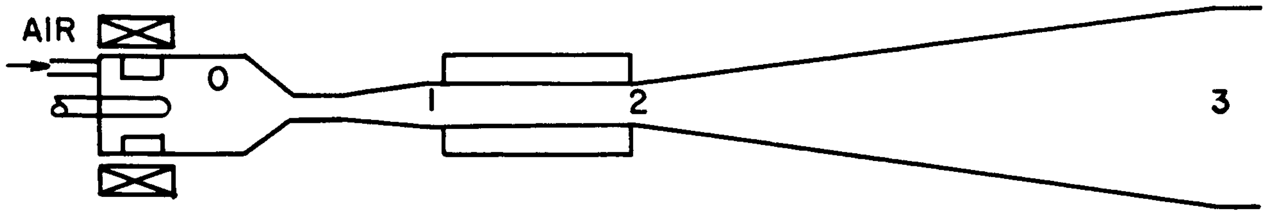

Figure 5.2-2 Arc Heater - DC MHD Accelerator Arrangement

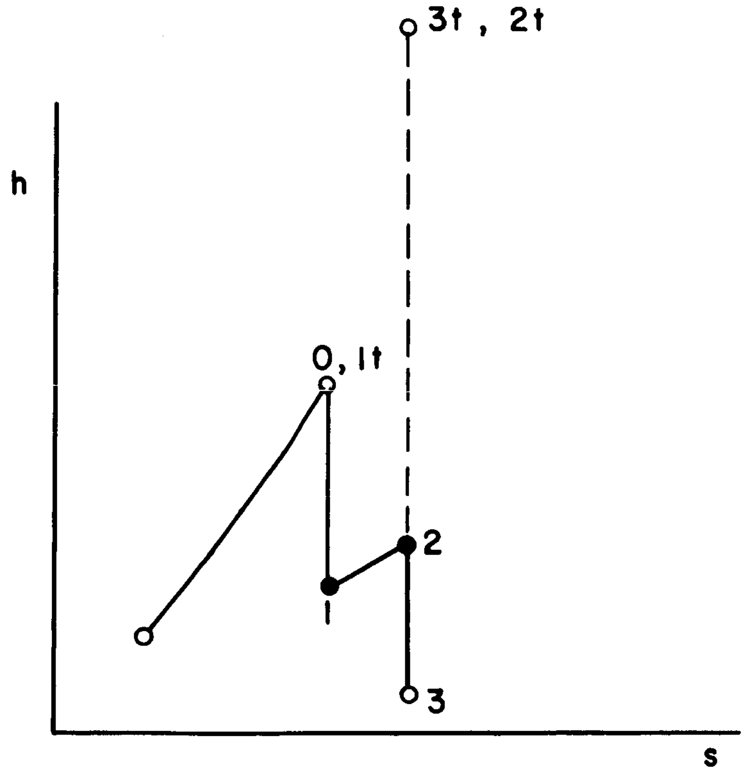

Figure 5.2-3 h-S Diagram with Notation

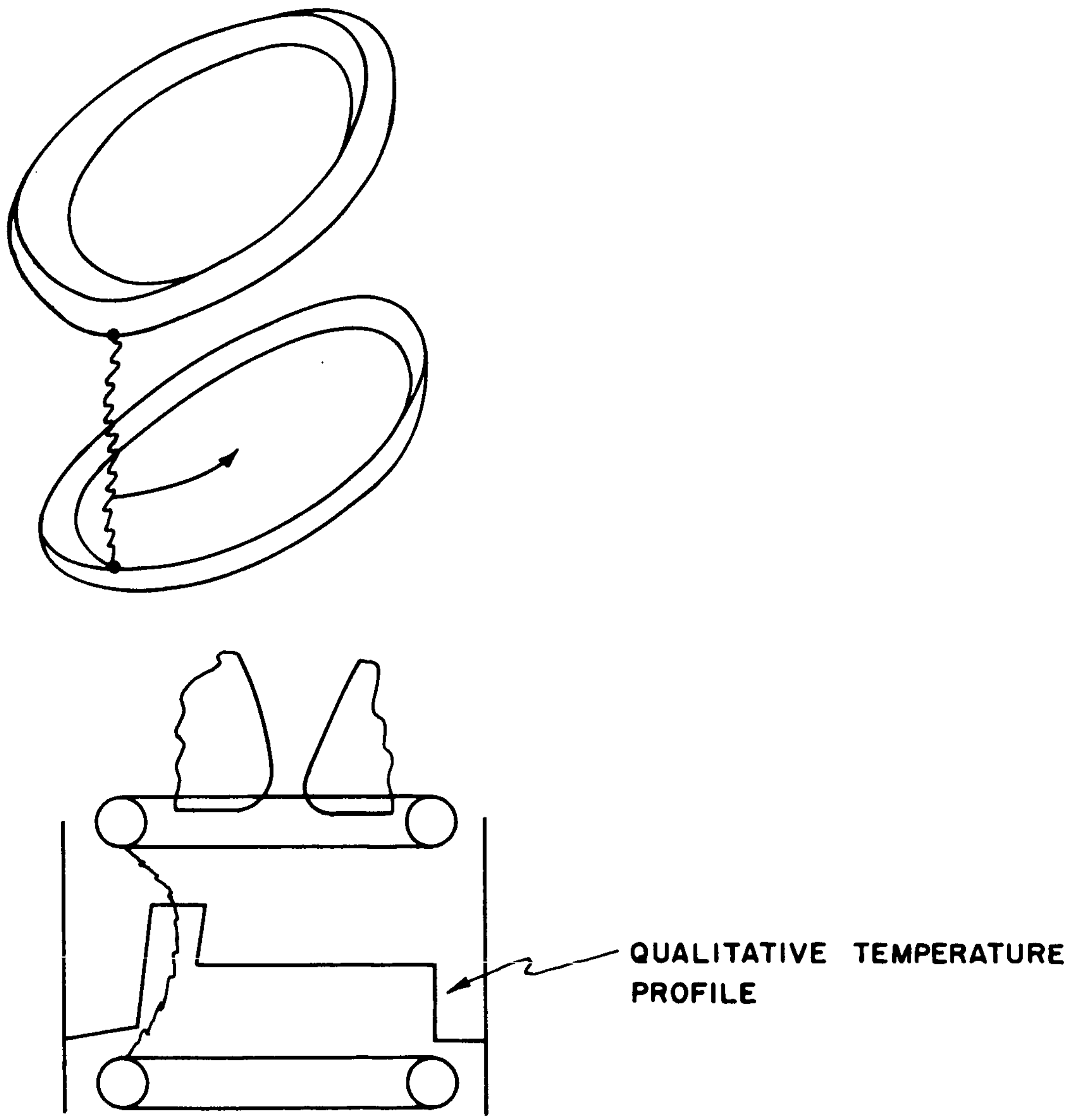

Figure 6.3-1 Thermal Profile, Cross Flow Heater

11. REFERENCES CITED

2.1.1.1 Bruning, A. M. (Arc Heater Department, Westinghouse Electric Corporation) personal communication.

2.2.1.1 Barger, R. L., Brooks, J. D. Beasley, W. D., NASA TN-D 716, National Aeronautics and Space Administration, March 1961.

2.2.1.2 Demetriades, S., and Ziemer, R. W., Energy Transfer to Plasmas by Continuous Lorentz Forces, Fourth Biennial Gas Dynamics Symposium, Proceedings, Northwestern University Press, Evanston, Ill., 1962.

2.2.1.3 Wood, G. P., et. al., Research on Linear Crossed-Field Steady-Flow D.C. Plasma Accelerators, AGARD Specialists Meeting, Rhode-Saint-Genise, Belgium, September 1964.

2.2.1.4 Hundstad, R. L., Holmes, F. A., and Tsu, T. C., Operating Experience with a Closed Loop Magnetohydrodynamic Facility, International Symposium on Magnetohydrodynamic Electrical Power Generation, Paris, France, July 1964.

2.2.3.1 John, R. R., and Bennett, S., Experimental Performance of a High Specific Impulse Arc Jet Engine, paper for presentation at the Fourth Electric Propulsion Conference (AIAA), Philadelphia, Pa., August 31, 1964.

2.2.3.2 Cann, G. L., Annular Magnetic Hall Current Accelerator, paper for presentation at the Fourth Electric Propulsion Conference (AIAA), Philadelphia, Pa., August 31, 1964.

3.1.1.1 Sarlitto, R. J., et. al., Development of High Enthalpy, High Power Arc Air Heaters, AF Flight Dynamics Laboratory, Research and Technology Division, Air Force Systems Command, Wright-Patterson Air Force Base, Ohio, RTD-TRD-63-4055, February 1964.

3.1.1.2 Stine, H. A., Watson, V. R., and Shepard, C. E., Effect of Axial Flow on the Behavior of the Wall-Constricted Arc, NASA TM X-54065, September 1964.

3.1.1.3 Bruning, A. M. (Arc Heater Department, Westinghouse Electric Corporation) personal communication.

3.1.1.4 Sarlitto, R. J., et. al., op. cit.

3.1.1.5 Smith, R. T., and Doyle, J. P., A 50-Megawatt Arc Heater: Scaling Parameters and Performance Predictions, AF Flight Dynamics Laboratory, Research and Technology Division, Air Force Systems Command, Wright-Patterson Air Force Base, Ohio, FDL TDR 64-91, August 1964.

3.1.1.6 Gowan, F. E. (NASA-Ames, Calif.) personal communication.

3.2.4.1 John, R. R., and Bennett, S., op. cit.

3.2.4.2 Cann, G. L., op. cit.

4.1.5.1 Boatright, W. B., et. al., Summary of Some of the Arc-Heated Hypersonic Wind-Tunnel Development Effort Underway at the Langley Research Center, Paper presented at the AGARD Specialists Meeting on "Arc Heaters and MHD Accelerators for Aerodynamic Purposes." Rhode-Saint-Genese, Belgium, September 1964.

4.1.5.2 Gowan, F. E. (NASA-Ames, Calif.) unpublished preliminary data.

5.1.1 Stine, H., Watson, V. R., and Shepard, C. E., Effect of Axial Flow on the Behavior of the Wall-Constricted Arc, paper presented to the AGARD Specialists' Meeting on Arc Heaters and MHD Accelerators for Aerodynamic Purposes, Rhode-Saint-Genese, Belgium, September 1964.

5.1.2 Cann, et. al., Basic Performance Limits of Coaxial Arc Gas Heaters, EOS Report RR-18, 30, November 1963

5.1.3 NAS1-3629-III

5.2.1 Joint Army, Navy, Air Force Interim Thermochemical Tables, Dow Chemical Co., Midland, Michigan, USAF Contract AF 33(616)-6149.

5.2.2 Frost, L. S., Conductivity of Seeded Atmospheric Pressure Plasma, Journal of Applied Physics 32, October 1961, pp. 2029-2036.

5.2.3 Moeckel, W. E., and Weston, K. C., Tech. Note 4265 Composition and Thermodynamic Properties of Air in Chemical Equilibrium, National Advisory Committee for Aeronautics, April 1958.

6.2.1 Sarlitto, R. J., et. al., op. cit.

6.3.1 Stine, H. A.; The Hyperthermal Supersonic Aerodynamic Tunnel, Intl. Union of Pure and Applied Chemistry, Butterworths, London, 1964.

6.2.2 Smith, R. T., and Doyle, J. P., op. cit.

6.2.3 Bruning, A. M., (Arc Heater Department, Westinghouse Electric Corporation) personal communication.

6.2.4 Wood, G. P., et. al., Research on Linear Crossed-Field Steady-Flow D-C Plasma Accelerators at Langley Research Center, NASA, paper for presentation at the AGARD Specialists' Meeting on Arc Heaters and MHD Accelerators for Aerodynamic Purposes, Rhode-Saint-Genese, Belgium, September 1964.

6.2.5 Smith, R. T., and Doyle, J. P., op. cit.

7.1.1 Sarlitto, R. J., et. al., op. cit.

7.2.1 Gowan, F. E. (NASA-Ames, Calif.) personal communication.

7.2.2 Bruning, A. M. (Arc Heater Department, Westinghouse Electric Corporation) personal communication.

7.12.1 Bruning, A. M., et. al., Progress Report #2, Contract NAS1-3629 (BDH), Task Order NAS1-3629-1, Westinghouse Electric Corporation, Trafford, Pa., August 1964.

7.22.1 Smith, R. T., and Doyle, J. P., op. cit.

7.26.1 Cann, G. T., et. al., Basic Research on Gas Flows Through Electric Arcs--Hot Gas Containment Limits, Office of Aerospace Research, United States Air Force Aerospace Research Laboratories (ARL 64-49), March 1964.

7.27.1 Stine, H. A., Watson, V. R., and Shepard, C. E., op. cit.

8.1.1.1 Ibid.

9.1.1.1 Brown, St. George Ambler, personal communication.

9.2.3.1 Hansen, C. F., "Approximations for the Thermodynamic and Transport Properties of High-Temperature Air" NASA R-50, 1959.